

## MASTER

### Time continuous interpolation of CCD signals for digital copiers

Werdler, L.J.B.

*Award date:*  
1994

[Link to publication](#)

#### **Disclaimer**

This document contains a student thesis (bachelor's or master's), as authored by a student at Eindhoven University of Technology. Student theses are made available in the TU/e repository upon obtaining the required degree. The grade received is not published on the document as presented in the repository. The required complexity or quality of research of student theses may vary by program, and the required minimum study period may vary in duration.

#### **General rights**

Copyright and moral rights for the publications made accessible in the public portal are retained by the authors and/or other copyright owners and it is a condition of accessing publications that users recognise and abide by the legal requirements associated with these rights.

- Users may download and print one copy of any publication from the public portal for the purpose of private study or research.
- You may not further distribute the material or use it for any profit-making activity or commercial gain

7177

TECHNICAL UNIVERSITY OF EINDHOVEN  
FACULTY OF ELECTRICAL ENGINEERING  
SECTION ELECTRONIC CIRCUIT-DESIGN

**Time continuous interpolation of  
CCD signals for digital copiers.**

L.J.B. Werdler (TUE id.nr. 273842)  
Venlo, july 1994

Section:

EEB (Electronic Circuit-Design)  
& Océ Nederland B.V.

Coaches:

Dr.Ir. P.C.W. Sommen (EEB)  
Dr.Ir. G.J. Rozing (Océ R&D)  
Ing. R.J. van der Meer (Océ R&D)

The faculty of electrical engineering of the Technical University  
of Eindhoven accepts no responsibility for the contents of this  
report.

## Samenvatting

Op de huidige kantoormarkt worden digitale copiers steeds belangrijker. De drie voornaamste onderdelen in een digitale copier zijn een scanner, een beeldbewerkingssysteem en een printer. In de scanner vindt de eigenlijke beeldbemonstering plaats door middel van de CCD sensor.

In de praktijk worden de uitgangssignalen van de CCD sensor bemonsterd en opgeslagen. Vervolgens worden digitale beeldbewerkingstechnieken toegepast om de opgeslagen data te interpoleren en daarmee resolutie conversie te kunnen realiseren of om te kunnen vergroten of verkleinen. Interpolatie van beeldinformatie kan ook bereikt worden door het blokvormige, amplitude gemoduleerde CCD signaal te filteren. Dit kan gerealiseerd worden door het blokvormige CCD signaal te converteren in een 'glad' tijdcontinu signaal dat de originele beeldinformatie benaderd. Het bemonsteren van dit signaal ('her-bemonstering' of 're-sampling') op een frequentie die hoger ligt dan de pixelfrequentie van het CCD-signaal maakt het mogelijk om te vergroten. Verkleinen ( of 'uit-zoomen') kan gerealiseerd worden door het gefilterde signaal op een lagere frequentie te bemonsteren.

Deze manier van interpoleren heeft verschillende voordelen. Zo kunnen resolutie conversies, zelfs met irrationele conversiefactoren, eenvoudig gerealiseerd worden door de juiste herbemonsterings-frequenties te kiezen. Een ander voordeel van het interpoleren met een laagdoorlaat filter is de onderdrukking van hoogfrequente ruis in de CCD signalen, waardoor de signaal/ruis verhouding verbeterd wordt.

Er zijn een aantal verschillende filter typen gesimuleerd als tijdscontinu interpolatie filter van CCD signalen. Twee filters bleken het meest aan de gestelde voorwaarden te voldoen: Een 7e orde Ulbrich-Piloty laagdoorlaat filter en een combinatie van een 4e orde Bessel laagdoorlaat filter met een 2e orde bandsper filter (Notch filter). Het Ulbrich-Piloty laagdoorlaat filter is uiteindelijk gebouwd en getest. Dit filter type heeft een bijna lineaire fase karakteristiek (dus ook een bijna constante groepslooptijd) in de doorlaatband en zorgt tegelijk voor een sterke onderdrukking van frequenties boven de doorlaatband. Door de bijna lineaire fasekarakteristiek blijft de vorm van randovergangen in de beeldinformatie zoveel mogelijk behouden. Het filter onderdrukt echter ook enigszins frequentiecomponenten onder de Nyquist frequentie, waardoor er scherpte verlies in de ingescande beelden optreedt.

Het Ulbrich-Piloty laagdoorlaat filter is ontworpen en geïmplementeerd in een verliesvrije LC ladder structuur vanwege de component ongevoeligheid en stabiliteit. Verschillende simulaties en tests hebben bewezen dat de toepassing van tijdscontinue analoge filters voor interpolatie en herbemonstering een bruikbare techniek is.

## Summary

In today's office market, digital copiers play a more and more important role. The three main parts of a digital copier are a scanner to sample the picture data, an image processing part and a printer. In the scanner, the actual sampling of picture information occurs in the CCD-sensor.

Normally, the output signals of the CCD-sensor are sampled and stored. Digital image processing techniques are used in order to interpolate the sampled data for resolution conversion or in order to zoom in or out. This resolution conversion basically means that pixel values of the signal are required at different discrete time than the synchronous pixel periods.

Interpolation of the picture information can also be accomplished by filtering the block pulsed amplitude modulated, CCD output signal. Here, this output signal is converted into a 'time continuous' smoothed signal that approximates the original picture information. Transformation to the time continuous domain offers the easiest way of interpolation because it removes artefacts as a result of the time discrete signal content. Sampling the smoothed signal ('re-sampling') at a higher sampling rate than the pixel rate of the CCD output signal, makes it possible to zoom in. Zooming out can be accomplished by re-sampling at a lower sampling rate.

This interpolation method has several advantages, for example resolution conversions, even with irrational conversion factors can easily be realised by choosing the right 're-sampling' rate. Another advantage of analog low pass filtering is the attenuation of high frequency noise in the CCD signal, which increases signal to noise ratio.

Several types of filters have been simulated for this purpose. Two filter types proved to meet most of the requirements: A 7th order Ulbrich-Piloty low-pass filter and a combination of a 4th order Bessel low-pass filter and a Notch filter. A seventh order Ulbrich-Piloty low-pass filter is implemented. This filter type is designed to have a small equiripple variation in the group-delay in the pass-band, maintaining a linear phase characteristic as much as possible. Due to this almost linear phase characteristic, the form of step-like picture information is preserved very well. On the other hand, the filter has some attenuation at frequencies below the Nyquist frequency, which decreases the sharpness of scanned images.

The Ulbrich-Piloty filter is designed and implemented in a lossless LC-ladder structure because of component insensitivity and stability. Several simulations and tests have proven that the application of time-continuous analog filters for interpolation and 're-sampling' of CCD-signals is a useful technique.

# Contents

1. Introduction .....	1
2. Digital scanning .....	2
2.1. The line CCD. ....	2
2.2. Signal-conditioning-electronics .....	5
2.3. Spatial discretisation .....	5
2.4. Visual effects .....	8
2.5. Optical filtering .....	9
2.5.1 Pixel area integration .....	9
2.5.2. Lense filtering .....	11
2.6. Fourier analysis of the scanning process .....	13
3. Resolution conversion .....	14
3.1. Digital interpolation .....	15
3.2. Switched capacitor filtering .....	16
3.3. Analogue filtering .....	17
4. Filter Design .....	18
4.1. Simulation of the optical filtering and sampling .....	18
4.2. Simulation of the CCD-signal .....	19
4.3. Analogue filter synthesis .....	21
4.4. Analogue filter types .....	22
4.5. Simulation results .....	23
5. Implementation .....	29
5.1. Ladder network decomposition .....	29
5.2. Pspice network-analysis .....	34
6. Tests .....	38
6.1. Frequency sweep .....	38
6.2. Test scans .....	38
6.2. Noise reduction .....	42
8. Conclusions .....	45
7. Recommendations .....	46
References .....	47

## 1. Introduction

In today's office market copiers play an important role. Besides the conventional analogue copiers, more and more digital copiers are developed. In an analogue copier the reproduction of an original is mainly based on optical and chemical processes. A sort of high resolution photographic picture is taken with a photosensitive plate and is then reproduced on paper using toner. The main difference with a digital copier is that digital copiers make use of electronic imaging (with less resolution), image processing and electronic printing techniques. Copy quality can be improved significantly using these techniques.

The three main parts of a digital copier are a scanner to sample the picture data, an image processing part and a printer. The actual sampling of picture information in a scanner occurs in the sensor. For this purpose one usually chooses CCD sensors. A CCD sensor is a photosensitive device that takes samples of a picture and converts it into an electronic signal. This electronic signal is then sampled by an Analogue-to-Digital converter and the sampled data is stored.

Most scanners and copiers have zooming capabilities. This means that a part of an original image is scanned and then printed at a larger scale. In digital scanners zooming can be achieved by different techniques.

The first method is to manipulate the lens system in the scanner. This method has some disadvantages. High mechanical and optical demands are imposed on the lens system. This will be reflected in higher cost prices, or bad performance properties. It also requires CCD sensors with different dimensions.

A second method of zooming is via digital interpolation; the CCD sensor takes samples of a picture and converts the information into a so called 'pulse-amplitude modulated' signal (see figure 5 in paragraph 5.2). The picture is digitized by sampling, quantizing and storing these amplitudes. In order to zoom in or out one can calculate values of extra sample points lying in between the stored sample points. For this purpose several interpolation algorithms can be applied as a form of image processing. These interpolation algorithms also make it possible to fit the scanner resolution to a different printer resolution. For example fitting a scanner resolution to a higher printer resolution means that additional pixels must be reconstructed out of the scanned image in order to reproduce the image with the printer. This is generally called resolution conversion. A drawback of digital interpolation are the use of extra memory and computation time, especially if resolution conversion with a irrational factors is needed.

It is also possible to reconstruct or interpolate the picture information electronically before quantisation and storage of the samples of the CCD signal. In this case the pulse-amplitude-modulated output signal of the CCD sensor is converted into a 'time continuous' smoothed signal that approximates the original picture information. More samples can then be taken from this smoothed signal by sampling at a higher sampling rate than the pixel rate of the CCD output signal, making it possible to zoom in. Zooming out can be realised by sampling at a lower sampling rate. In the latter case one has to take into account that extra aliasing artefacts can be introduced and must be dealt with.

The objective of the work described in this report was to examine the possibility and feasibility of interpolating CCD information in the analogue domain, so that it can be re-sampled for resolution conversion. In this report the design and synthesis of an analogue, time-continuous, interpolating filter is described. Also experimental results of a hardware implementation are presented.

## 2. Digital scanning

In a flatbed- or rollerfeed scanner a picture is sampled line by line. As mentioned before, the information of a line is sampled with a so called line-CCD. In both flatbed and rollerfeed scanners, the original is illuminated and optics (lenses, filters, mirrors etc. ) are used to project the original onto the sensor. A complete scan is made by either moving the CCD-sensor (flatbed scanner) or moving the original (rollerfeed scanner). In figure 1. a schematic overview of these scanning methods is shown.

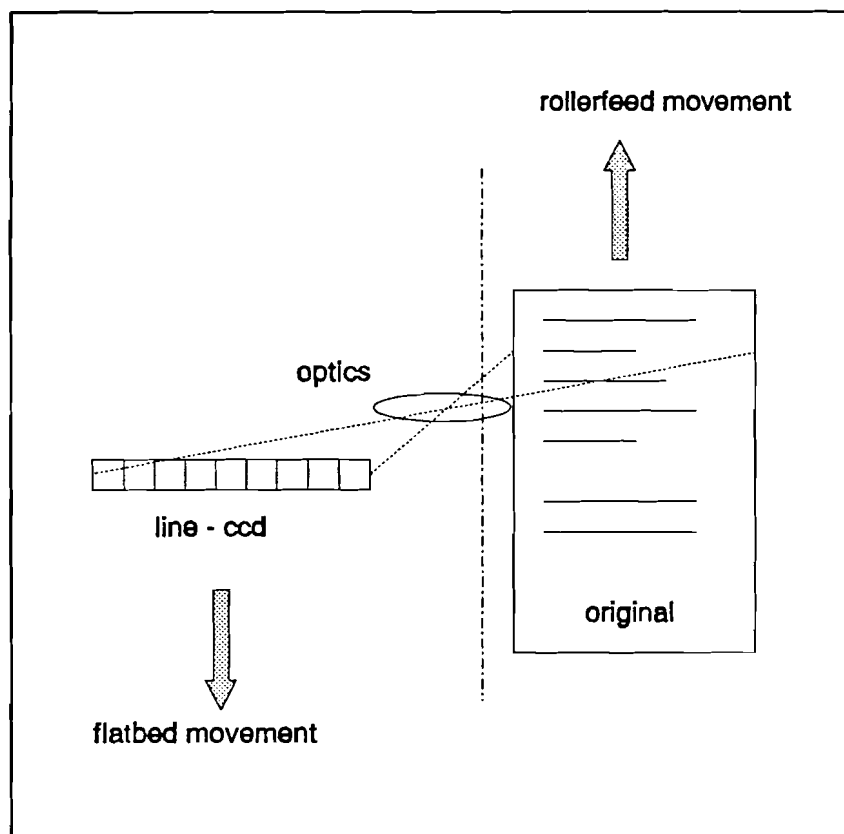


Figure 1. Two methods for scanning a picture with a line-CCD.

### 2.1. The line CCD.

CCD is an abbreviation of 'Charge Coupled Device'. A line-CCD contains an array of photosensitive elements (photosites or pixels) with corresponding MOS capacitors.

In the photodiode structure, an N+ region is implanted in the P-type substrate in order to form a PN diode. Due to a positive overlying polysilicon gate, the diode is 'reverse biased' and a space-charge zone is created. An illuminated pixel converts photons to negative charge in the 'floating' N+ zone.

The time interval in which incoming photons are converted into charge, is called the exposure period. This time interval can be seen as an integration period of the light energy, collected in a pixel area. Here the spatial discretisation of the picture information takes place.

After this period, the charge of the photosites is shifted towards the readout register by depleting a

neighbouring diode more heavily so that an electric field is induced which transfers the charge. The readout register consists of an array of MOS capacitors (potential well). In figure 2. an overview of a line-CCD is given.

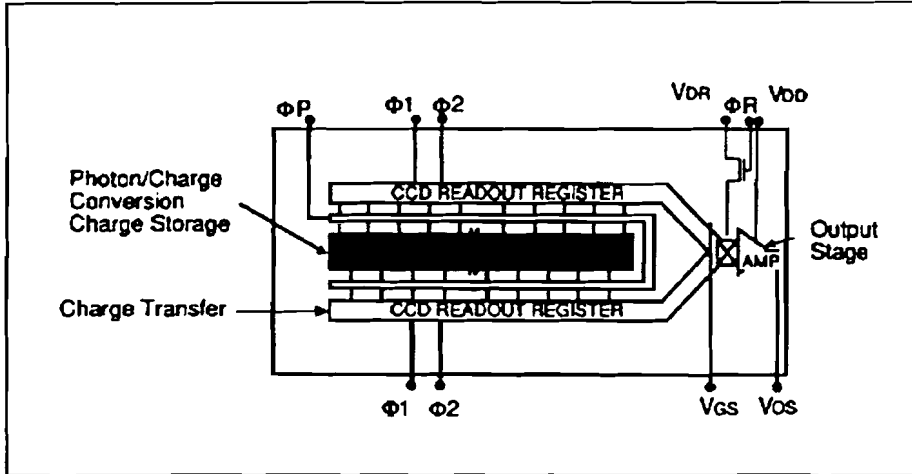


Figure 2. Functional block diagram of a line-CCD.

The packets of accumulated charge are transported sequentially along the potential wells. One can say that at this moment the readout register (transport register) of the CCD is used as an analogue shift register, shifting the charge information of every pixel sequentially through the array of potential wells, towards the output stage. This is shown in figure 3.

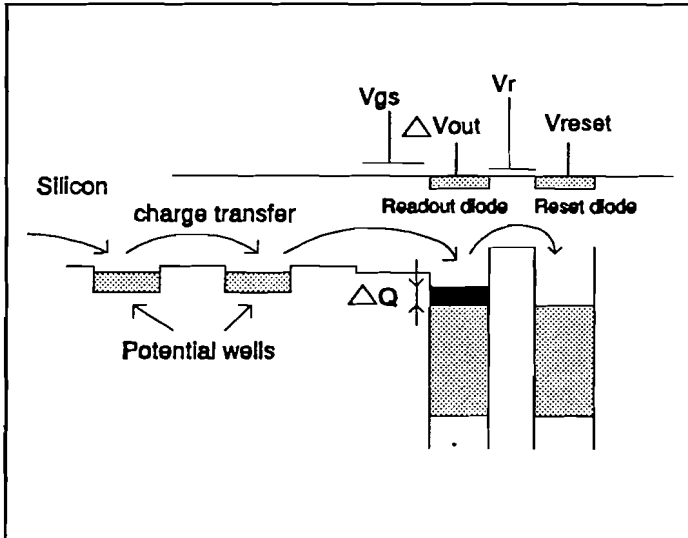


Figure 3. Charge transfer along the potential wells.

At the output stage, a charge-to-voltage conversion takes place, followed by amplification. After each charge to voltage conversion the potential well of the output amplifier must be cleared, before charge information of the next pixel can be fed to the output. During this 'reset' period the output voltage of the CCD is set by the capacitive feed-through of the reset voltage. After the reset period, the potential well of the readout diode returns to a high impedance state until it is filled with the charge representing information of the next pixel. During this period the readout diode is said to be 'floating' [1]. Figure 4 schematically shows the output signal of a CCD. The charge representing the pixel information that is shifted to the output stage causes the output voltage of the readout diode to be smaller than the 'floating diode voltage'.



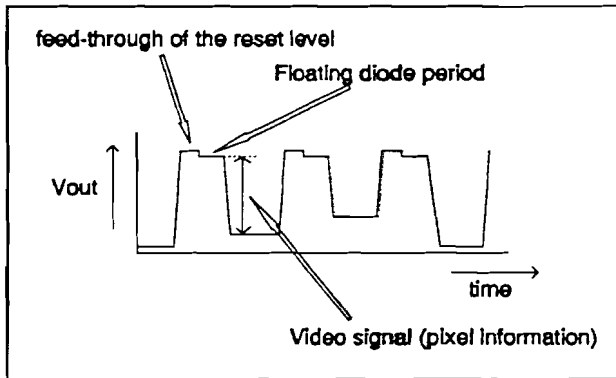


Figure 4. CCD output signals.

At this point, spatially distributed line information has been converted into a time-distributed voltage signal. This signal can be seen as a pulse-amplitude-modulated signal. In figure 5 this conversion is schematically shown. Figure 5 also shows that a CCD pixel being illuminated, for example pixel 1, will have a lower corresponding pulse-amplitude than a non-illuminated pixel (for example pixel 3.) due to negative charge (electrons).

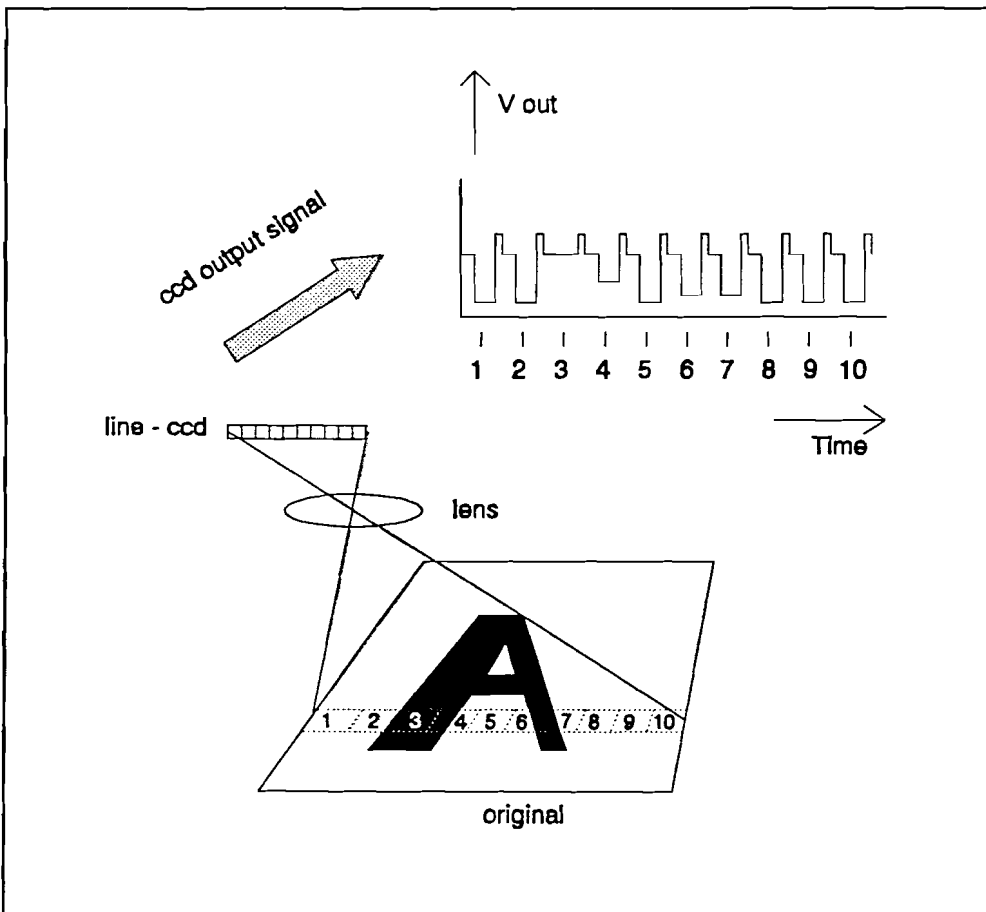


Figure 5. Converting spatial discrete information into a form of pulse-amplitude-modulated information.

## 2.2. Signal-conditioning-electronics

The output signal of the CCD-sensor, as in figure 5, has to be manipulated by signal-conditioning-electronics. The main task of this signal conditioning electronics is to adapt the range of the CCD-output to the range of the Analogue-to-Digital Converter (ADC). The ADC is used to convert the analogue video-signals into digital signals that can be stored in digital memory. The signal-conditioning-electronics can also invert the CCD-output signals, in order to create a high positive voltage of a pulse corresponding to an illuminated pixel and a low positive voltage corresponding with a non-illuminated pixel.

Figure 6 shows a part of an actual output signal of the signal-conditioning-electronics. In this example, the pixel frequency of the CCD-output is approximately 12 MHz.

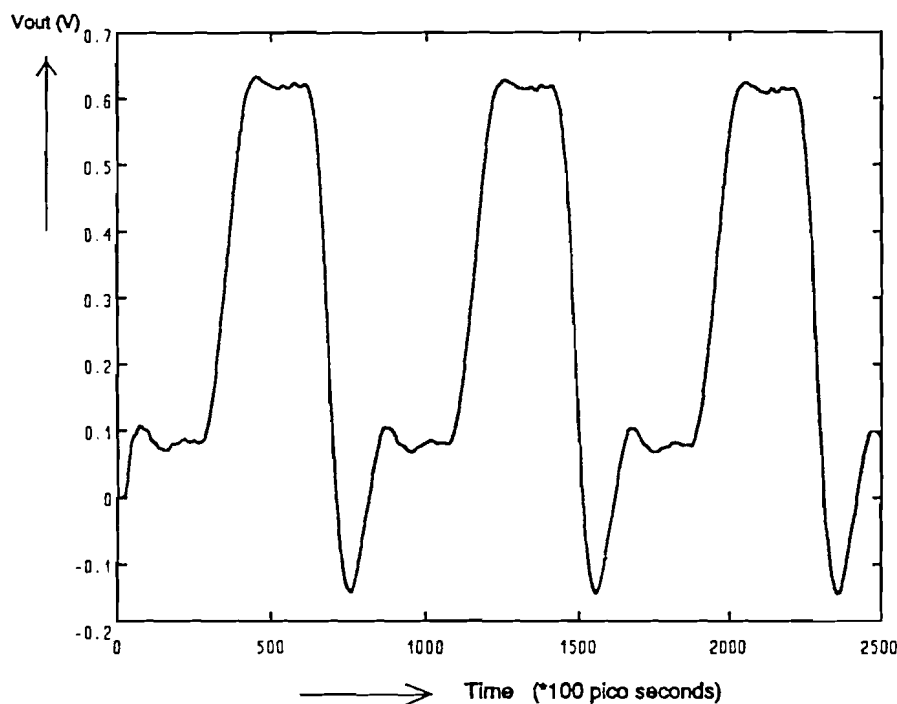


Figure 6. Part of an CCD output signal processed with signal conditioning electronics.

## 2.3. Spatial discretisation

When spatial picture information is sampled, the number of samples per unit length is referred to as the "addressability" and is often given in dots per inch (dpi). The resolving power or "resolution" of a scanning system is determined by the dimensions of the photosensitive areas of the CCD-pixels and the lense properties. The addressability of a CCD-sensor is given by the distance between the centers of two pixels, also called the 'sample pitch' and is generally not the same as the resolution.

The addressability refers to spatially distributed information. Transfer functions of signals in the spatial frequency domain, are generally referred to as Modulation Transfer Functions (MTF).

The process of sampling time-distributed signals with Dirac pulses at sample rate  $f_s=1/T_s$  (with  $T_s$  being the sample pitch) can be mathematically described as the multiplication of the input signal  $(x(t))$  with a train of Dirac-pulses (represented by  $s_s(t)$ ).

$$x_{\delta}(t) = \sum_{k=-\infty}^{\infty} x(kT_s) \delta(t - kT_s)$$

with:

$$x_{\delta}(t) = s_{\delta}(t) x(t)$$

$$s_{\delta}(t) = \sum_{k=-\infty}^{\infty} \delta(t - kT_s)$$

1.

In the Fourier domain (Fourier transformation is denoted as  $F(\cdot)$ ) these formulas are transformed into:

$$X_{\delta}(\omega) = F(x_{\delta}(t)) = F(x(t) s_{\delta}(t)) = F(x(t)) \otimes F(s_{\delta}(t))$$

by definition:  $X_{\delta}(\omega) = S_{\delta}(\omega) \otimes X(\omega)$

$$S_{\delta}(\omega) = F(s_{\delta}(t)) = f_s \sum_{k=-\infty}^{\infty} \delta(\omega - k\omega_s)$$

$$X_{\delta}(\omega) = f_s \sum_{k=-\infty}^{\infty} X(\omega - k\omega_s) = \frac{1}{T_s} \sum_{k=-\infty}^{\infty} X(\omega - k\omega_s)$$

2.

A multiplication of time-distributed signals comes down to the convolution (denoted as  $\otimes$ ) of their frequency spectra of these signals. As a result of this convolution, the Fourier transform of the multiplication  $x_{\delta}(t)s_{\delta}(t)$  is the spectrum  $X(\omega)$ , repeated at frequencies  $k\omega_s$  with  $k = \dots, -2, -1, 0, 1, 2, \dots$ . If the spectrum of  $X(\omega)$  is bounded between  $-(\omega_s/2)$  and  $+(\omega_s/2)$ , the repeating frequency bands of  $X_{\delta}(\omega)$  do not overlap. This implies that in principle each of these frequency bands can then be used to restore  $x(t)$  out of  $x_{\delta}(t)$ . If the spectrum is not bounded between  $-(\omega_s/2)$  and  $+(\omega_s/2)$ , the repeating frequency bands of  $X_{\delta}(\omega)$  overlap and aliasing will occur. In that case  $X(\omega)$  cannot be restored without introducing restoration errors.

The term  $(f_s/2)$  is often referred to as the Nyquist frequency and is equal to:

$$f_{Nyquist} = \frac{f_s}{2} = \frac{\omega_s}{4\pi}$$

3.

The sampling theory for time-distributed signals can also be applied for spatially distributed information. The highest spatial frequency in one direction (x or y), that can be reproduced correctly in theory, is the one-dimensional spatial Nyquist frequency and is defined as:

$$f_{Nyquist} = \frac{1}{(2 * T_s)}$$

4.

with  $T_s$  representing the sample pitch in one direction.

The process of sampling a 2-dimensional image  $o(x,y)$  with dirac-pulses can be derived in an equivalent way:

$$g(x, y) = o(x, y) s_{\delta_x \delta_y}(x, y)$$

$$s_{\delta_x \delta_y} = \sum_{n=-\infty}^{\infty} \sum_{m=-\infty}^{\infty} \delta((x-nT_x), (y-mT_y))$$

$$\delta(x, y) = 0, \quad x \neq 0 \vee y \neq 0$$

$$\delta(x, y) \rightarrow \infty, \quad x=0 \wedge y=0$$

$$\int_{-\infty}^{\infty} \int_{-\infty}^{\infty} \delta(x, y) dx dy = 1$$

5.

Here  $g(x,y)$  describes the original  $o(x,y)$  sampled with 2-dimensional dirac pulses that are equally spaced in the x-direction with sample pitch  $T_x$  and in the y-direction with sample pitch  $T_y$ .

The Fourier transform of  $g(x,y)$  is equal to the 2-dimensional convolution of  $s_{\delta_x \delta_y}$  and the Fourier transform  $o(x,y)$ . This is shown in the following formulas:

$$O(\omega_x, \omega_y) = \int_{-\infty}^{\infty} \int_{-\infty}^{\infty} o(x, y) e^{-j(\omega_x x + \omega_y y)} dx dy$$

6.

$$\begin{aligned} S_{\delta_x \delta_y}(\omega_x, \omega_y) &= \int_{-\infty}^{\infty} \int_{-\infty}^{\infty} s_{\delta_x \delta_y}(x, y) e^{-j(\omega_x x + \omega_y y)} dx dy \\ &= \frac{1}{T_x T_y} \sum_n \sum_m \delta(\omega_x - n\omega_{s_x}, \omega_y - m\omega_{s_y}) \end{aligned}$$

7.

$$\begin{aligned} G(\omega_x, \omega_y) &= S_{\delta_x \delta_y}(\omega_x, \omega_y) \otimes O(\omega_x, \omega_y) \\ &= \frac{1}{T_x T_y} \sum_n \sum_m O(\omega_x - n\omega_{s_x}, \omega_y - m\omega_{s_y}) \end{aligned}$$

8.

Formula 8 shows that the 2-dimensional Fourier spectrum of the original picture  $o(x,y)$  sampled with dirac pulses, is equal to the 2-dimensional spectrum  $O(\omega_x, \omega_y)$  repeated at  $(n\omega_{s_x}, m\omega_{s_y})$  with  $n = \dots, -2, -1, 0, 1, 2, \dots$  and  $m = \dots, -2, -1, 0, 1, 2, \dots$

If the Fourier transform  $O(\omega_x, \omega_y)$  has spectral components only for  $-\omega_{s_x}/2 < \omega_x < \omega_{s_x}/2$  and  $-\omega_{s_y}/2 < \omega_y < \omega_{s_y}/2$ , the repeating 2-dimensional frequency bands will not overlap and each of these frequency bands in principle contains the same picture information. This means, just like the one-dimensional case, that each of these frequency bands could be used to reconstruct the original picture  $o(x,y)$ .

## 2.4. Visual effects

If an original picture has spatial frequency components that are higher than the Nyquist frequency of the CCD-sensor, aliasing will occur. This implies that these frequency components are 'folded back' to frequencies that are smaller than the Nyquist frequency. These extra low-frequent signals can cause visually disturbing patterns.

Next to aliasing there's also the phase effect that occurs due to sampling. The phase effect becomes most disturbing as the frequency of the original signal approximates the Nyquist frequency. The phase effect can be caused by the phase difference between the original frequency and the Nyquist frequency or by the phase difference between an original frequency and an aliased frequency. An example of the phase effect is the following; An original picture consists of a rastered photograph. Suppose that the spatial frequency in one dimension of the raster pattern is almost equal to the spatial Nyquist frequency which is set by the CCD. The phase difference of the raster and the pixel locations of the CCD then varies with a very low frequency. This becomes visible as a low-frequent pattern in the reproduced picture. This phase effect is shown in the low frequent pattern in the bottom-left part of figure 7.

So called 'Moire patterns' are caused by both the phase effect and aliasing. In figure 7 several effects of Moire patterns are visualised.

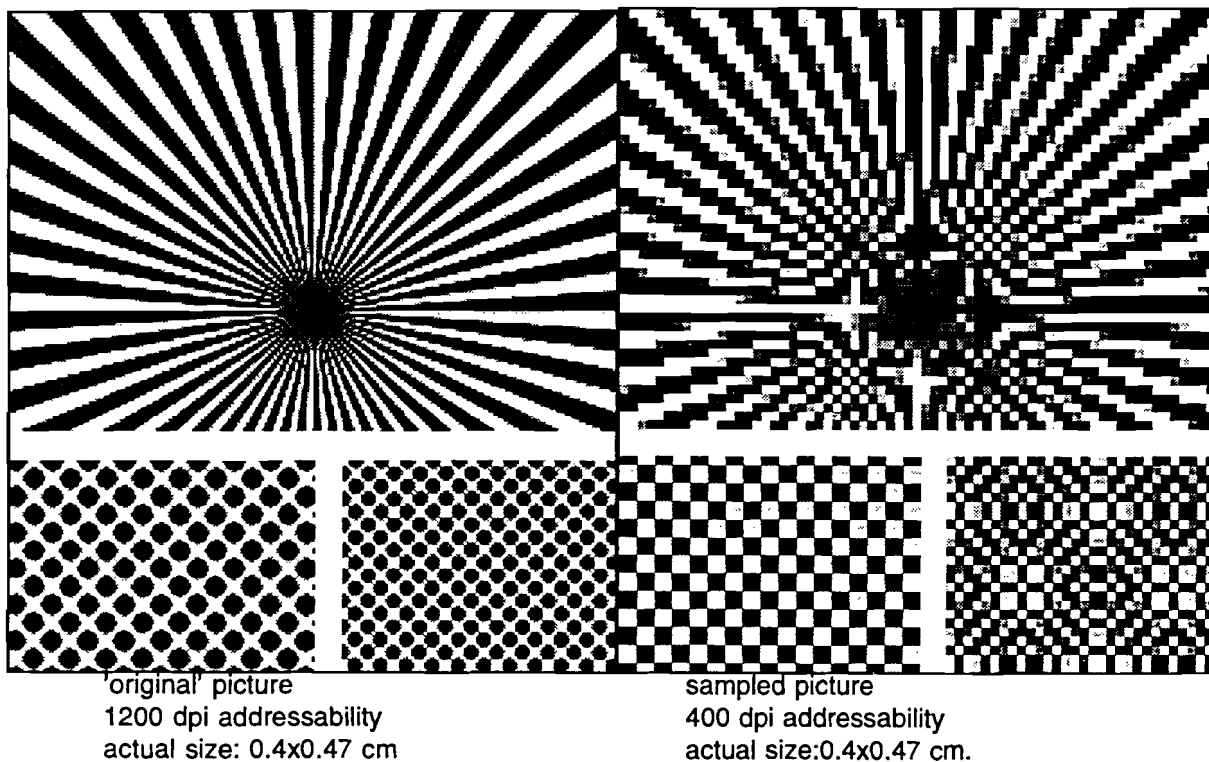


Figure 7. Moiré patterns caused by aliasing and phase effects.

The 'original' picture on the left is digitally stored with an addressability that is significantly higher (1200 dpi) than the addressability of the sampling process in this example (400 dpi). The low frequent patterns in the middle of the top part of the figure are caused by both the phase and aliasing.

It will be clear that in some cases these Moiré patterns are undesirable for high quality digital copiers.

## 2.5. Optical filtering

To prevent disturbing Moiré effects in the scanning process, one should ideally low-pass filter the original picture before the discretisation phase, thus in the optical path. Ideally this low-pass filter must have a pass-band from 0 to the Nyquist frequency and a stop band starting at the Nyquist frequency. However, this is not achievable completely. Fortunately, there are two processes in that already act as an optical low-pass filter. These processes are area integration by the photosensitive pixel areas of a CCD-sensor and low pass filtering properties of lenses. The behaviour of a CCD-sensor and the lense-filtering in the (spatial) frequency domain are characterized by their Modulation Transfer Functions (MTF).

### 2.5.1 Pixel area integration

The first process of low-pass filtering in the optical path is area integration by the CCD-pixels. In figure 8 the sample pitch  $T_x$  and photosensitive area, related to the geometric definitions of the CCD sensor, are shown.

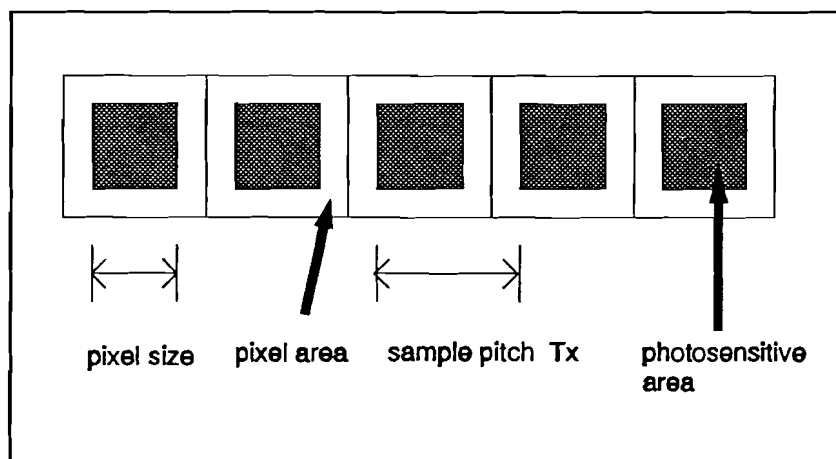


Figure 8. Geometric definitions in a CCD-sensor.

As mentioned in chapter 2.1, a pixel integrates the amount of light energy that enters its photosensitive area during the exposure period. This integration of light information over an area is equal to the average amount of light energy, that enters the area during the exposure period, multiplied with the size of the area. Since the size of the photosensitive area is fixed, the integrated light information is equal to the average light information scaled by a fixed factor. In the CCD-sensor this 'averaging' process occurs at the photosensitive areas, that are spaced with the sample pitch, only.

The combination of area integration (photosensitive area) and the sample pitch in one dimension is schematically shown in figure 9.

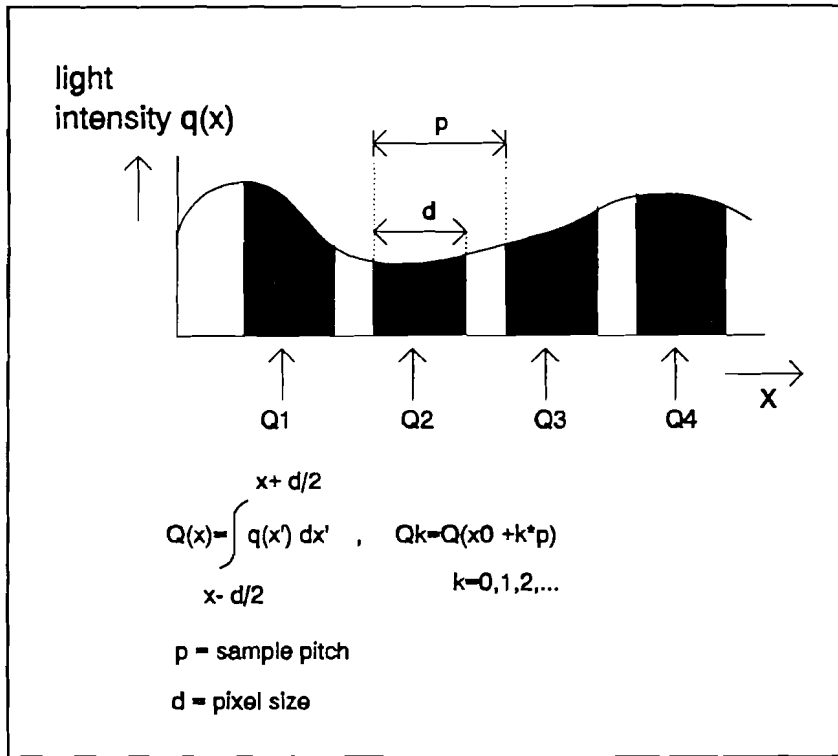


Figure 9. Discretisation of the spatial information.

The function  $q(x,y)$  describes the amount of light energy that is converted into charge at location  $(x,y)$ , during the exposure period. Here, this light energy, integrated over an area  $d^2$ , is described as the function  $Q(x,y)$ :

$$Q(x,y) = \int_{y-\frac{d}{2}}^{y+\frac{d}{2}} \int_{x-\frac{d}{2}}^{x+\frac{d}{2}} q(x',y') dx'dy'$$

9.

$Q(x,y)$  is equal to the 2-dimensional convolution of  $q(x,y)$  with the convolution kernel  $D(x,y)$

$$Q(x,y) = \int_{-\infty}^{\infty} \int_{-\infty}^{\infty} \int_{-\infty}^{\infty} \int_{-\infty}^{\infty} D(x-\tau_x, y-\tau_y) q(x,y) dx dy d\tau_x d\tau_y$$

$$D(x,y) = 1 \quad |x| \leq +\frac{d}{2}, \quad |y| \leq +\frac{d}{2}$$

$$D(x,y) = 0 \quad |x| > +\frac{d}{2}, \quad |y| > +\frac{d}{2}$$

10.

A line CCD takes samples of  $Q(x,y)$ , at the pixel locations  $(x_0+kp, y_0)$  only, with  $k=0,1,2,\dots$  and  $p$  the sample pitch, so these samples can be described as:

$$Q_k = Q(x_0 + kp, y_0)$$

11.

For sampling a single line with a line-CCD, the vertical position is assumed to be constant and is noted here as  $y_0$ . In the frequency domain, looking in the x direction only, the one-dimensional MTF of this pixel area integration results in a so called 'sinc' function (with a phase shift of  $\omega d/2$ ). This can be seen by calculating the 2-dimensional Fourier transform of  $Q(x, y_0)$ :

$$\begin{aligned} Q(\omega_x, y_0) &= Q(\omega_x, 0) \int_{-\infty}^{\infty} D(x, y) e^{-j\omega_x x} dx \\ &= Q(\omega_x, y_0) \int_{-\frac{d}{2}}^{\frac{d}{2}} e^{-j\omega_x x} dx \\ &= Q(\omega_x, y_0) (e^{+j\omega_x \frac{d}{2}}) d \left( \frac{1 - e^{-j\omega_x d}}{j\omega_x d} \right) \\ &= Q(\omega_x, y_0) (e^{+j\omega_x \frac{d}{2}}) d \frac{\sin(\omega_x d)}{(\omega_x d)} \end{aligned}$$

12.

A practical example is a line CCD having a photosensitive area size which is 60% of the CCD pixel area (60% of the sample pitch in the x-direction and 100% of the sample pitch in the y-direction). This example is used for figure 10.

### 2.5.2. Lense filtering

The second form of optical filtering is the lense. Tuning the lenses somewhat out of focus will cause extra attenuation of high spatial frequencies.

The filter properties of the lense system can be described by the so called point spread function (PSF). This function represents the two dimensional spreading (or smoothing) of a 'Dirac-like' dot of light over an area. When looking in the x-direction only, as for the line-CCD, the corresponding line spread function can be found by integrating the point spread function in the y-direction;

$$LSF(x) = \int_{-\infty}^{\infty} PSF(x, y) dy$$

13.

In the frequency domain the transfer characteristics of the lense are described with it's Modulation Transfer Function. A rather general analytic approximation of this MTF has been found to fit a large number of cases [6] and is of the form:

$$H_{LSF}(j\omega) = \int_{-\infty}^{\infty} LSF(x) e^{-j\omega x} dx = e^{-\left(\frac{1}{2\pi} |Z_0 \omega|\right)^n}$$

14.

Here n is a constant and  $Z_0$  is the smoothing parameter of the function. Often a good approximation



of the MTF of lenses is achieved for  $n=1$ . For the line spread function this results in the so called 'Lorentz' function, which is the inverse Fourier transform of the MTF:

$$LSF(x) = \frac{1}{\pi} \cdot \frac{Z_0}{Z_0^2 + x^2}$$

15.

The transfer function  $H_{lsf}$  can be seen as a low pass filter in the 1-dimensional spatial domain. There are only two filter operations before the sampling process of the CCD sensor, namely the area integration by the CCD pixels and low-pass filtering by the lens characteristics. Since the dimensions of the photosensitive areas of the CCD-sensor are fixed, aliasing effects due to sampling can only be reduced by the lens-filter operation. The properties of the lens filtering can be controlled by choosing the right type of lens and tuning the focussing depth. In most cases, lenses with a line spread function that can be approximated by the Lorentz function, are able to reduce most of the aliasing effects by tuning the focussing depth, thus controlling parameter  $Z_0$ .

Using lenses as a form of optical low-pass filtering, aliasing effects should be reduced as much as possible, on the other hand too much attenuation of frequencies below the Nyquist frequency must be avoided. In figure 10 an example of an MTF plot of the combination of this lens filtering and the CCD pixel area integration is shown. This MTF is equal to  $|H_{lsf}(\omega)H_{a_i}(\omega)|$  and can be seen as MTF of the optical imaging system.

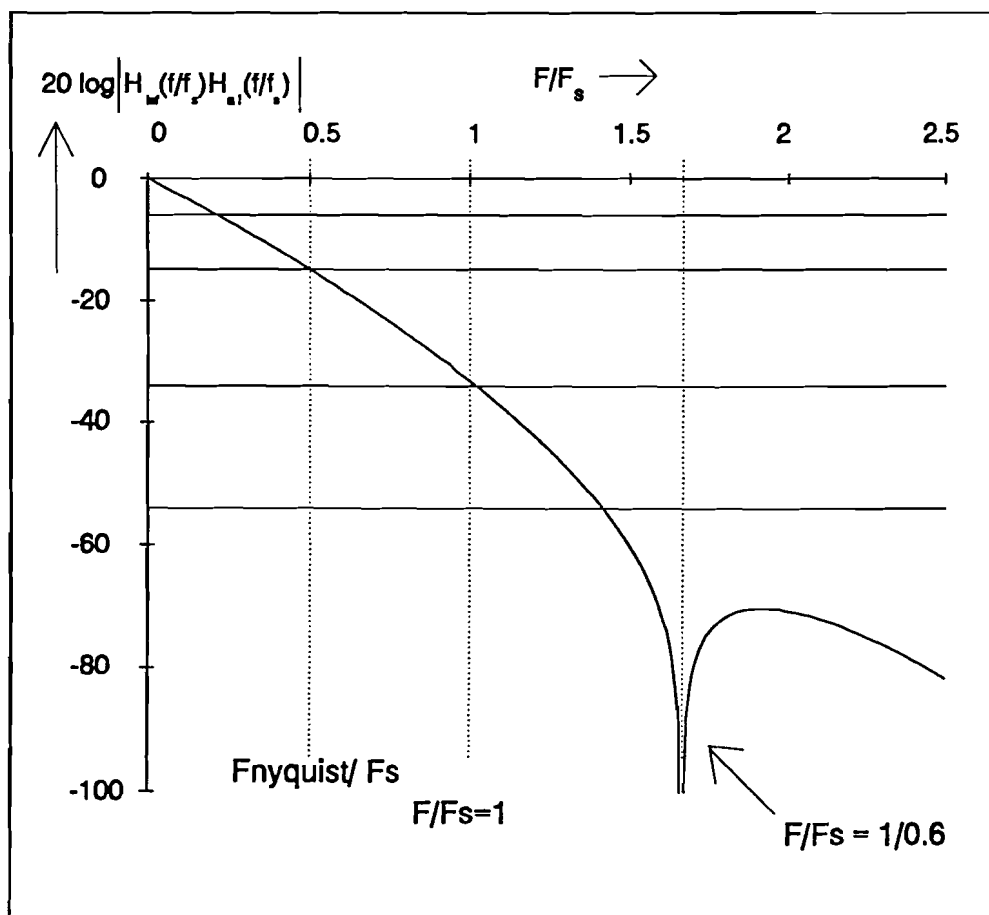


Fig.10. The one-dimensional MTF of a lens in combination with area integration of a CCD sensor.

(*photosensitive area: 60% of pixel area*)  
*addressability: 200 dpi*  
*Z0 : 50 μm*)

## 2.6. Fourier analysis of the scanning process

The scanning process can be divided into several stages. The power spectra of the intermediate signals are shown in figure 11. Spectrum A shows the power spectrum of an original picture and the power spectrum after optical filtering (lense filtering and area integration). Spectrum B represents the spectrum after sampling. Since the image is sampled with spatial sample frequency  $F_s$ , the sampled image information is limited to the Nyquist frequency  $F_N$ .

The output of a CCD sensor is a pulse-amplitude modulated signal with reset-periods. This comes down to making the spectrum periodic by repeating the spectrum B followed by the spectral filtering as shown in C. In this example the pixel pulses have a 50 % duty cycle. A 50% duty cycle of these pixel pulses can be seen as sampled pixel information that is held for 50% of the clock period. Due to this block-pulsed signal, the periodic spectrum is attenuated by a sinc-function. The dirac pulses in spectrum C represent the DC-component of the reset pulses and the first harmonic frequencies of both the reset pulses and the block-pulsed pixel signals. The part of the spectrum C that represents the optical filtered picture information is shaded.

If one wants to apply resolution conversion, the CCD signal must be 're-sampled' with a frequency that is not equal to the pixel frequency ( $F_s$ ). In this case all frequency components above the Nyquist frequency ( $F_N$ ) add no extra information and must be attenuated sufficiently before 're-sampling' the CCD signal. If not attenuated sufficiently, they can cause extra aliasing effects at the 're-sampling' stage. In the special case of re-sampling at exactly the pixel frequency which is usually done in digital copiers, no extra aliasing artefacts are created and attenuation of frequency components above the Nyquist frequency is not required in principle.

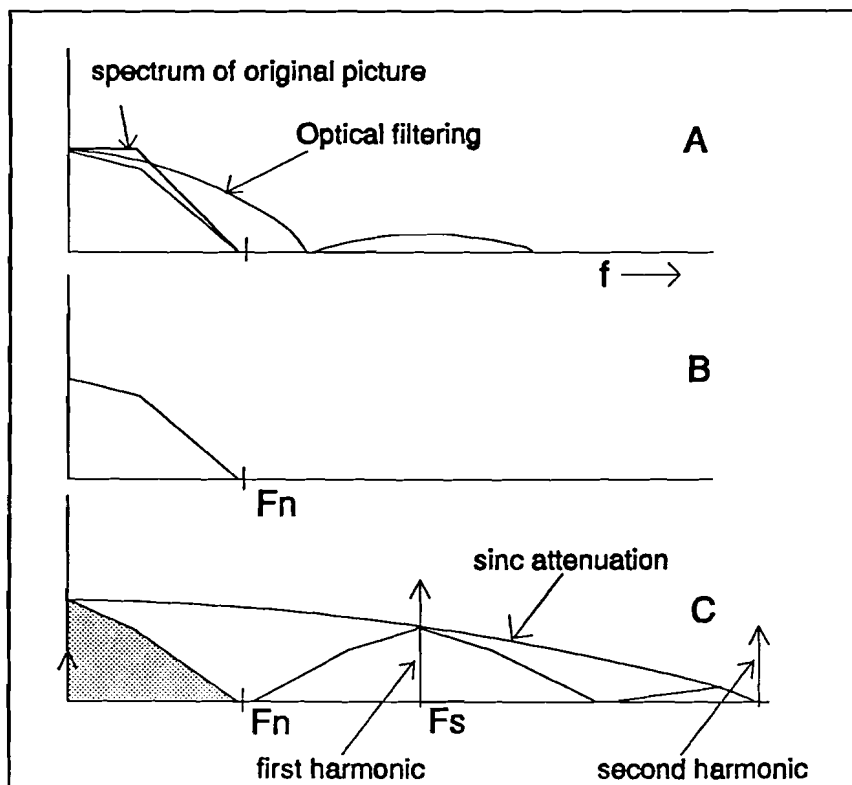


Figure 11. Signal spectra of an original and optical filtered picture (A), the sampled picture information (B) and the CCD output signal (C).

### 3. Resolution conversion

Converting information density of a scanned image to a higher or lower density is generally called resolution conversion. This can be applied in order to fit the addressability of a scanner to the addressability of a printer, or in order to zoom in or out. Here pixel information of pixels lying in between scanned pixels must be reconstructed or interpolated. In order to reconstruct more detailed picture information, in practice several interpolation techniques are used. Three types of interpolation techniques can be realised. One can apply filter techniques in continuous time domain or the discrete time domain having analogue or quantised amplitudes. In the following tabel an overview of these types is given.

**Tabel I** Several types of interpolation techniques

	Digital Amplitude	Continuous Amplitude
Discrete Time	1. Digital Interpolation	2. Switched-Capacitor filters
Continuous Time	-----	3. Analogue filters

In the case of flatbed or rollerfeed scanners, the vertical addressability can be controlled with the speed of the line CCD in the scanning direction. Decreasing the scanning speed of a line CCD makes it possible to take more samples per unit length. Thus controlling the vertical sample pitch, in the scanning direction results in a higher vertical addressability.

However, the vertical dimension of the photosensitive area of the CCD is fixed. This means that if the vertical sample pitch is set smaller than the vertical component of the photographic area of the line CCD, pixel areas of the subsequent pixels in the scanning direction will overlap and a sort of interlacing occurs. This interlacing is shown in figure 14.

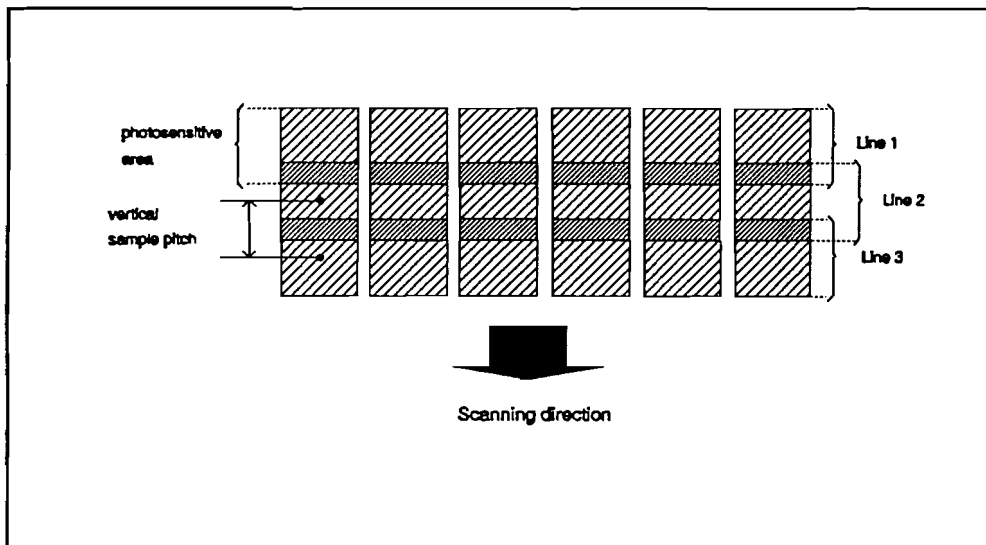


Figure 14. interlacing with a line CCD.

In this way, scanning with a higher vertical addressability can be achieved, although low-pass filtering is still caused by the pixel area integration in both the vertical and horizontal direction.

The horizontal addressability of the rollerfeed or flatbed scanners is set by the number of pixels of the line-ccd. Since this number is fixed, a one-dimensional interpolation technique must be applied to increase the addressability. In the case of vertical interlacing, extra information of the original picture is scanned. In the case of interpolation in the horizontal direction no extra picture information is gathered. Here the information of additional pixels, lying in between the sampled pixels, is only approximated by interpolation techniques.

Using interpolation techniques it is also possible to fit the scanner addressability, for example 400 dpi, to a different printer addressability, for example 600 dpi. This is called resolution conversion.

### 3.1. Digital interpolation

In digital scanners first the picture is digitized. Suppose a line-CCD samples a line with a fixed spatial sample rate. The CCD output consists of a block-pulsed signal with amplitudes representing the pixel charges. This blockpulsed CCD output-signal is sampled with its puls-frequency, quantised and stored. The result is a set of samples representing the picture information. This process is called the digitizing phase.

After the digitizing phase, digital interpolation techniques can be applied to restore extra pixel information, lying in between the stored sample points. For example, first order curve fitting between every two succeeding pixels (linear interpolation) can be applied. In the following figure an example is given of linear interpolation, applied for zooming in with a factor 3/2.

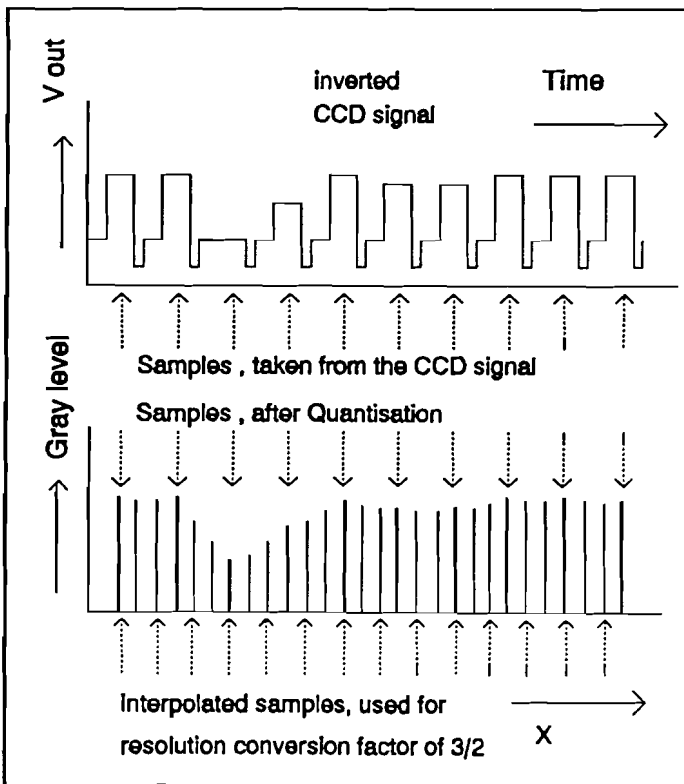


Figure 12. Digital linear interpolation (spatially discrete)

This method of interpolation can be applied in a one dimensional or a two dimensional way. Two dimensional interpolation can be used for images that are scanned with a fixed horizontal and vertical addressability. A typical numerical implementation of this method is given in the next figure. In this example the interpolation is applied in order to zoom out. Here, the resolution conversion factor in both the horizontal direction and the vertical direction is  $3/4$ . This implies zooming out with a factor  $3/4$ .

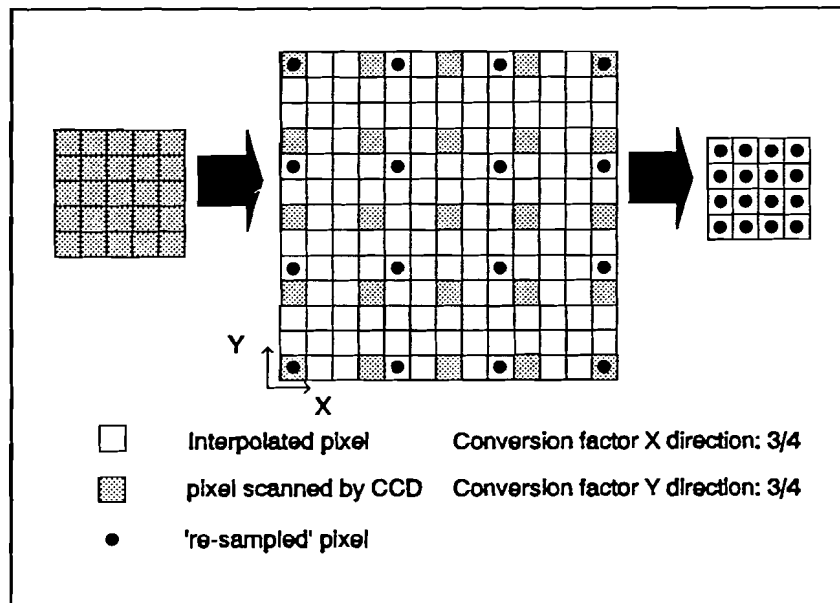


Figure 13. 2-Dimensional digital interpolating.

Some drawbacks of interpolating image information digitally however are the use of extra memory and the computation time in the case of the implementation of figure 13. Another drawback is the fact that interpolated information is based on digitally stored, thus quantised, picture information, introducing extra quantisation errors. Next to this, the exact sample moment must be well chosen in order to avoid sample-errors caused by overshoots or cross-talk in the block-pulsed CCD-signal. High frequency noise components in the CCD signals can also cause quantisation errors and therefore an extra analogue low-pass pre-filter should be used.

### 3.2. Switched capacitor filtering

One can also apply filtering techniques in the discrete time domain but operating with analogue (non-quantised) amplitudes. Filters of this type make use of sample & hold circuits and can be designed for an Finite Impulse Response (FIR) or an Infinite Impulse Response (IIR) [8]. In tabel 1. these filters are of type 2.

Some discrete-time filters of type 2 (FIR or IIR filters) for resolution conversion have been developed recently [4, 12]. These filters take samples of the pixel amplitudes in the CCD signal and reconstruct signals a time discrete intervals between CCD pixels. When applying these filters in digital scanners several pre-cautions must be taken:

1. The switched capacitor filters take samples of the input signal. If the input signal is distorted by high frequent noise, sample errors are made. In order to attenuate this high frequent noise in the block pulses of the CCD signal, one has to use an extra analogue low-pass (pre-)filter.

2. The exact sample moment must be well chosen in order to avoid sample-errors caused by overshoots in the block-pulsed CCD-signal.

3. The time-discrete output signal of the FIR or IIR filters ('staircase' signals) must be 'smoothed' by low-pass (post-)filtering it in the case of re-sampling at a frequency that is not equal to the pixel frequency.

A drawback of these filters is the use of many delay sections (sample & hold) operating at clockfrequencies, that are at least several times the pixel rate of the CCD output signal. Since this pixel rate can be in the order of 10 to 20 MHz or more, high demands are imposed on the applied digital electronics, regarding clock feed-through and stability. Some filters of this type have been implemented [4, 12] in 2 $\mu$ -CMOS. The filters that are described in [4, 12] have a maximum internal clock-rate of 50MHz. This implies that for example a CCD signal with a pixel rate of 20 MHz can be interpolated with 2.5 discrete time intervals per pixel.

### 3.3. Analogue filtering

Interpolation of the picture information can also be accomplished by analogue low pass filtering of the block pulsed, amplitude modulated, CCD output signal. This means that here the actual interpolation occurs before sampling the CCD signal.

In this way a 'time continuous' smoothed output signal approximating the original picture information is made. In fact, here the picture information, lying in between the CCD pixels, is interpolated in the time continuous domain. Samples of the smoothed signal ('re-sampling') can then be taken at sample rates which are practically free to choose (irrational zoom factors) and are in fact limited by the maximum sample rate of the Analogue-to-Digital converter. Another advantage in comparison with digital interpolation or switched capacitor filtering is the suppression of high frequency noise in the CCD signal. In figure 15 the principle of this interpolation method is shown.

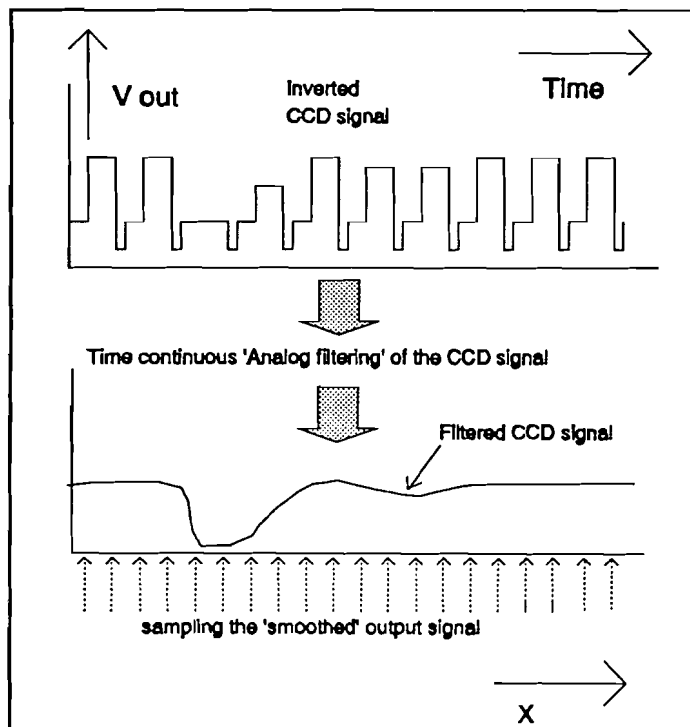


Figure 15. 'Low pass' filtering the CCD signal and 'resampling' it.

## 4. Filter Design

Because of the several advantages of analogue interpolation filtering for re-sampling compared to digital interpolation or switched capacitor filtering, an analogue filter is designed and implemented. Since the process from optically sampling an image to storing or printing the image is very complicated, several simulations of the performance of analogue filtering in the scanning process have been made in order to design an analogue 'smoothing' filter. For this purpose the simulation programs 'MATLAB', 'SIMULINK', 'KHOROS' and 'CANTATA' are used. Matlab is a so called 'High Performance Numeric Computation and Visualisation Program' and consists of a large number of mathematical tools. The SIMULINK software can be used in combination with MATLAB. SIMULINK acts as a visual programming interface in which several (MATLAB-) function blocks can be connected to each other. This is of great use when simulating a complex system containing many complex transfer functions.

KHOROS consists of mathematical tools and many image processing tools. This software can also be used in combination with a visual programming environment, called CANTATA. This software is UNIX based and operates on workstations, making it possible to handle large amounts of data. This can be useful for calculating 2-dimensional convolutions of large images and complex convolution kernels.

Using these simulation programs, several parts of the scanning process have been simulated. The scanning process consists of an optical filtering part, the spatial discretisation process by the CCD, a conversion from spatial information into time distributed signals, a filtering or interpolation part and the process of 're-sampling' of the time distributed signals.

To be able to simulate the scanning processes a realistic representation of an original picture must be made. An original picture can contain a photograph, a raster or text. Images containing text exhibit many step-like responses. Images that contain photographic information are sensitive to noise while rastered figures may create Moiré patterns. For the simulations of the scanning process these 'high resolution' original pictures can be approximated by representing them with an addressability that is several times higher than the addressability of the CCD sensor, in order to avoid discretisation errors. On the other hand this addressability must be limited because of the computation time and available memory that are needed for the simulations.

### 4.1. Simulation of the optical filtering and sampling

In the scanning process the original picture is optically filtered prior to sampling. The modelling of this optical filtering has been described in 2.2 and 2.3. The two major factors that determine the optical filtering are the lense system and the pixel area integration of the CCD sensor.

The smoothing of the picture due to the lense system can be simulated by a 2-dimensional convolution of the original picture with a so called 'convolution kernel'. This convolution kernel is determined by the Lorentz function described in 2.3.

The effects of the area integration can be simulated by the 2 dimensional convolution of the lense-filtered picture with the convolution kernel that describes the area integration. This convolution kernel is represented as a square area with a constant amplitude. The result of the convolution is stored as the optically filtered picture. In the following figure an example of the convolution kernels for lense filtering (Lorentz) and area integration are shown.

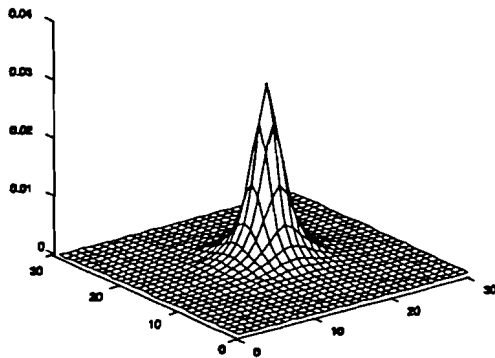
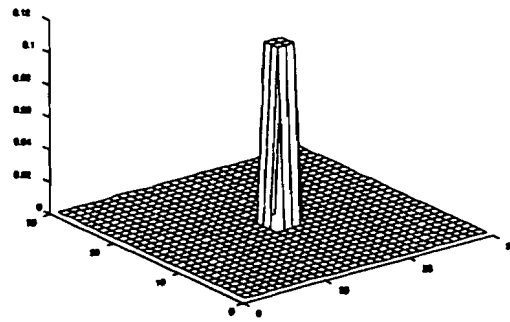


Figure 16. a The convolution kernel of a Lorentz function.



b. The convolution kernel of area integration.

In this example, the original picture is represented with an information density of 1200 dpi. The addressability, in both horizontal and vertical direction, of the simulated area-CCD is set to 240 dpi. This means that the sample pitch of the CCD-sensor is equal to a distance of  $(1200/240)=5$  datapoints. Here the smoothing parameter  $Z_0$  is set to 50 micrometer. A photosensitive area of 36% (In the horizontal and vertical direction is the pixel size equal to 60% of the sample pitch) is then simulated with a convolution kernel of 3x3 datapoints, that is shown in figure 16b.

The optically filtered picture is stored with the same high addressability as the stored original picture. The actual sampling by the CCD sensor can now be simulated by sampling the optical filtered picture with the CCD-sample pitch. The result is a picture with the same addressability as the CCD sensor. This picture represents the image information that the CCD sensor would collect in a real scanning system.

## 4.2. Simulation of the CCD-signal

The 2-dimensional spatially sampled image is converted into a 1-dimensional datastream that describes the pixel information of the image line by line. The output signals of the CCD are simulated with SIMULINK, using transfer functions in the Z-domain describing the blockpulses that are amplitude modulated by the pixel information.

In the simulations, the CCD-signals were described with  $N_i$  datapoints per pixel-period. Each block-puls containing information of a pixel is simulated with  $P_2$  datapoints, each reset period with  $(P_3-P_2)$  datapoints and each floating diode period with  $(N_i-P_3)$  datapoints.

In figure 17 a form of a pixel period in relation to the datapoints is shown.



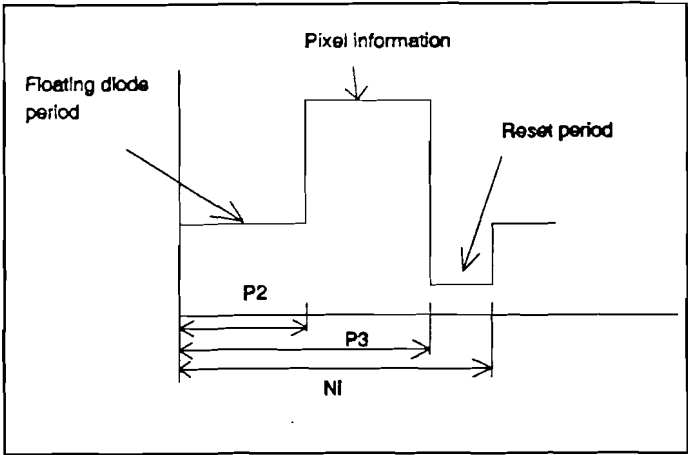


Figure 17. A pixel period simulated with Ni datapoints.

The digital transfer functions that are used to create these pulses out of the stored pixel information, are shown in the following figure. The figure is a so-called workspace that is used in SIMULINK.

The data-input 'in\_1' represents the information of the picture. The Discrete Transfer Function (1/1) is used in 'in\_1' to convert the stored picture data ('in\_1') into a time-discrete data stream representing the data of the picture scanned line by line. The complete ccd-signal is created by adding the train of reset pulses to the block-pulsed pixel signals. This resulting signal is then fed through a second order Butterworth low-pass filter in order to simulate the overshoot in the block-pulses of the output channel of the CCD-sensor.

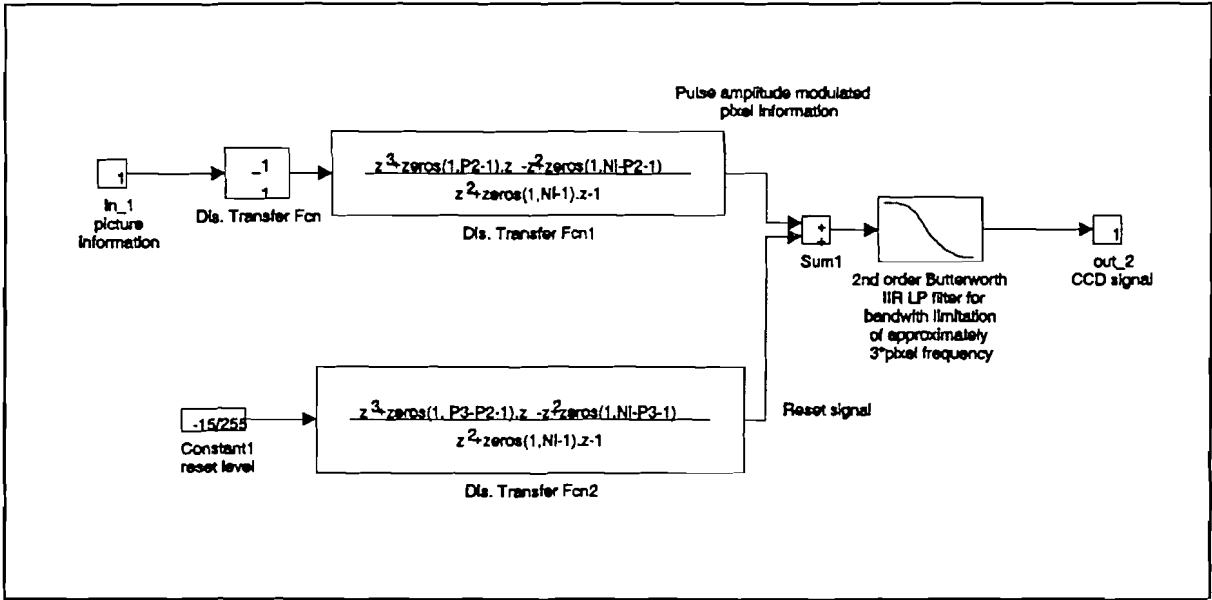


Figure 18. A SIMULINK workspace for simulating the conversion of pixel information into ccd-signals.

Examples of the different simulation steps in this workspace are schematically shown in figure 19.

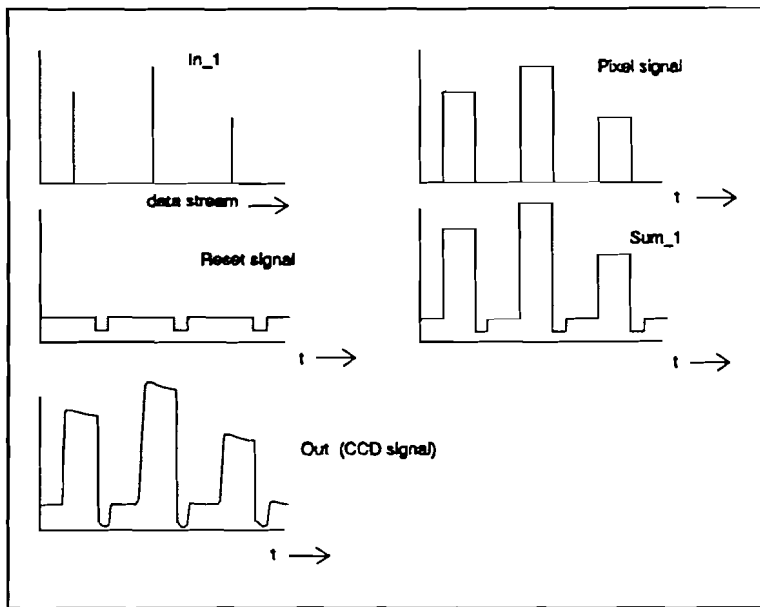


Figure 19. Examples of signals in the workspace of figure 18.

### 4.3. Analogue filter synthesis

For the synthesis of an analogue 'smoothing' filter, several (pre-)conditions have to be made:

1: All frequency components above the Nyquist frequency ( $F_n$ ) add no extra information and must be attenuated sufficiently before 're-sampling' the CCD signal. If not attenuated sufficiently, they could cause extra aliasing effects at the 're-sampling' stage. Special attention must be given to the following, relatively large harmonic frequencies that are higher than the Nyquist frequency :

\*: The first harmonic of the amplitude-modulated blockpulses that represent the pixels, must be attenuated sufficiently in order to create a smooth CCD-signal. For example a picture containing low frequent high light levels, that is sampled with a CCD-sensor will result in a train of block pulses at the clock-frequency with relatively large pulse amplitudes. The original picture information is low frequent and the blockpulses must be smoothed in order to approximate this low frequent information.

\*: The 'Reset' pulses (clock frequency) in the CCD signal must also be attenuated sufficiently. In the frequency spectrum the repeating reset pulses are represented as a DC-component, a first harmonic frequency component at the pixel frequency and several higher harmonics, which are very large compared to the baseband spectrum. The DC-component of the reset pulses in the ccd-signal can be attenuated by controlling the offset voltage. The first harmonic of the reset pulses is found at the pixel-frequency. It has an amplitude that is not related to the pixel amplitudes and is practically constant (see also figure 11).

2: 'step like' picture information must be preserved as much as possible and on the other hand 'ringing' must be avoided as much as possible. 'Ringing' is the effect that becomes visible in the step response of a low-pass filter that is underdamped. The step-like information can very often be found in sharp contrasted pictures (for example text-originals).

In the following picture the effect of ringing in the horizontal direction is made visible. Here the horizontal line information of a text-original is filtered with a Chebyshev low-pass filter having a cut off characteristic that is too steep at the Nyquist frequency in the baseband spectrum.

Step like information can be preserved as much as possible by designing a filter with a linear phase characteristic in the passband. This means that the group delay of the frequency components in the passband is constant.



Figure 20. An example of the 'Ringing' effect.

3: In the ADC, 8 bit quantisation is used. This implies that the dynamic range is limited to 48 dB (256 'gray levels'), and the 'noise floor' for stochastic signals, due to quantisation noise, is  $20 \cdot \log(2^8/0.5) = 54$  Db below the maximum value of the 8 bit representation of the gray levels. If a block-pulsed CCD signal is distorted with (high frequent-) noise, samples of the block pulses will have sample errors due to this. The application of time-continuous low-pass filters causes high frequency noise in the CCD signal to be suppressed. A low-pass filtered CCD signal will cause less sample errors caused by noise frequencies above the Nyquist frequency.

4: The Nyquist frequency of the CCD-output is in the order of several MHz, so the filter must be designed for these high frequencies.

#### 4.4. Analogue filter types

It may be clear that a perfect low pass filter cannot be realised, so a best fit to the pre-conditions has to be made. There are several well known filter types that have been optimized to specific filter characteristics. These filter types can be compared for application as analog interpolation filter, in relation to the pre-cautions that are described in paragraph 4.3. The following filter types are evaluated:

- The Cauer (elliptic) filter is often used in the audio world for low pass filtering of 'time discrete' signals. These Cauer filters have one or more pairs of zeros in the s-plane on the imaginary axis, and several poles at the left half. In general, using these filters one can realise a very steep roll off in the frequency spectrum. However, the locations of the poles and zeros have to be chosen carefully in order to achieve an admissible (non-linear) phase characteristic.

In fact, a Cauer low-pass filter can be seen as a combination of one or more Notch filters (band reject filters) and a standard low pass filter, such as Butterworth or Chebycheff low-pass filters. Several of these filter combinations are simulated in SIMULINK as 'smoothing filters':

A combination of a single Notch filter for sufficient attenuation of relatively large frequency components at the clock-frequency and one of the following low-pass filter types for attenuation of frequencies above the Nyquist frequency:

- a Butterworth low pass filter which is designed to have a maximum flat passband.
- a Chebycheff low pass filter for faster 'roll off' allowing some ripple in the passband of the power spectrum.
- a Bessel low-pass filter for preserving step like information optimally by causing a constant group delay.

A filter type that realises an optimal combination of a steep roll off in the power spectrum with an almost constant group delay within the passband, is a so called Ulbrich-Piloty low-pass filter [2]. This filter is designed to have a small equiripple variation in the group delay in the passband, retaining a linear phase characteristic as much as possible. The almost linear phase characteristic of an Ulbrich-Piloty filter preserves the form of step-like information very well. Compared to Bessel low-pass filters, the equiripple variation in the group delay causes the Ulbrich-Piloty filter to have a much steeper roll off in the power spectrum than Bessel filters of the same order.

In SIMULINK a workspace is created to simulate the behaviour of the previously described filters in a scanning process. In figure 21. this workspace is shown. Here the block 'CCD' represents the workspace that converts the sampled picture information into a CCD output signal (see paragraph 4.2). The output of this block is fed through several filter types in order to simulate the time continuous 'smoothing' of the CCD-signals. In the figure two of these filter types , an Ulbrich\_Piloty filter and a combination of a Notch filter and a Bessel filter, are shown.

The output blocks 'loccd', 'lo3' and 'lo4' in the figure store the results of the different simulation blocks in the workspace-output. The outputs 'lo3' and 'lo4' can then be sampled at a certain sample pitch in order to simulate the 're-sampling' process.

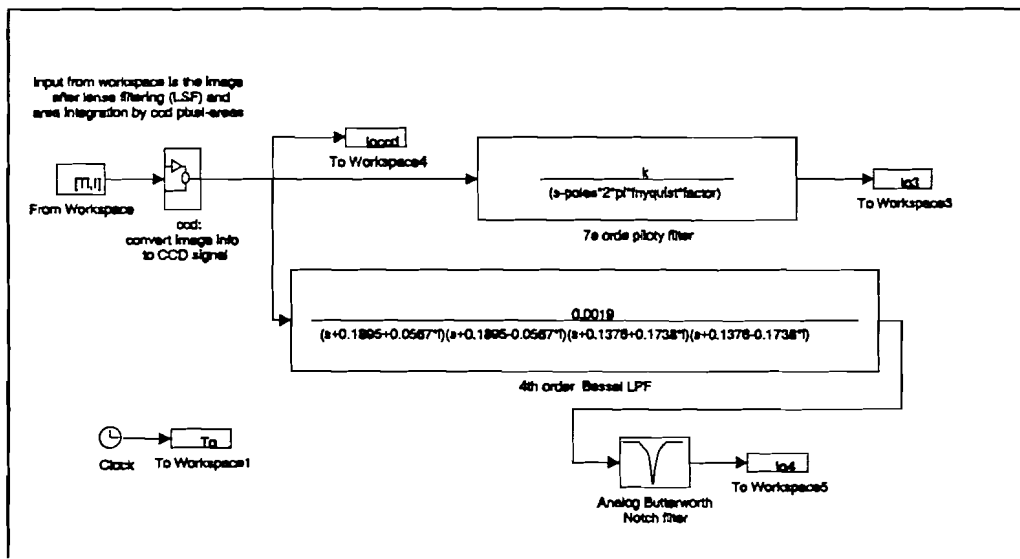


Figure 21. Simulink Workspace simulation 'time-continuous' filtering of CCD signals.

#### 4.5. Simulation results

Several filters that are described in chapter 4.3. are compared by simulating their behaviour in workspaces as described above. The differences in the behaviour of the filters are mainly judged by comparing responses to step-like picture information mainly visually and checking the attenuation of frequency components above the Nyquist frequency. The minimal order that was needed for each filter type has also been taken into consideration.

After comparing several simulation results, two types for filtering the CCD-signal proved to answer most of the precautions:

**A 7th order Ulbrich-Piloty low-pass filter**, designed for an equiripple group delay within a frequency range of 0 to  $f_{\text{Nyquist}}$ . The filter preserves step-like information well and causes no ringing artefacts. The frequencies above the Nyquist frequency are attenuated sufficiently if 8-bit quantisation is applied. The Ulbrich Piloty low-pass filter that is described here, has the following specifications:

The transfer function has 7 poles and no zeros. In the s-plane for a normalised passband range of 0 to 1 rad/sec, the poles are located at :

```

p1= -0.333144
p2= -0.327777+i*0.357891
p3= -0.327777-i*0.357891
p4= -0.305975+i*0.703901
p5= -0.305975-i*0.703901
p6= -0.235504+i*1.022953
p7= -0.235504-i*1.022953

```

This filter has a group delay with a ripple of 0.69 % in the frequency range 0- $f_{ref}$ . In this case the filter parameter  $\tau_0$  is equal to :

$$\tau_0 = \text{group delay} * 2\pi f_{ref} = 3.6$$

$$\delta = (0.69\%) * \tau_0$$

16.

If the filter is applied for a passband of for example 10 MHz, the group delay will result in 57.3 ( $\pm 0.69\%$ ) nsec. For more detailed information and tabulated poles of Ulbrich-Piloty filters, see [2 page 44-47].

In figure 22 the amplitude and phase characteristics of this filter type are shown. It can be seen that frequencies below the Nyquist frequency are also attenuated. In this figure the filter was designed for a CCD-pixel-frequency of 10 MHz.

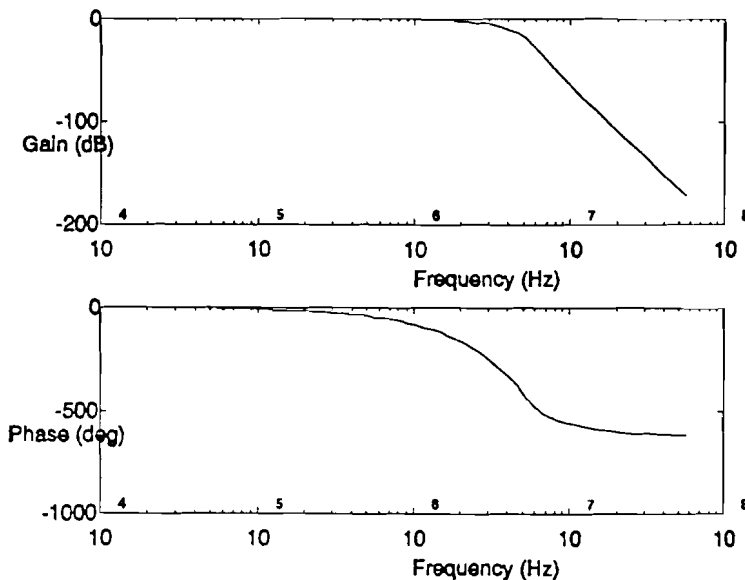
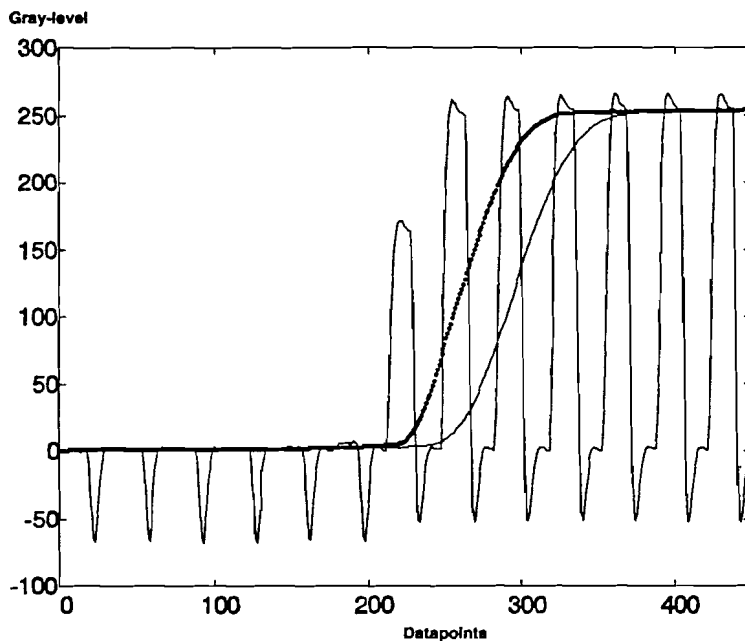


Figure 22. Amplitude and phase characteristics of the Ulbrich-Piloty filter.

In the following figure the results of a (transient) simulation are shown. The CCD-output signal is shown together with the corresponding time continuous output of a 7th order Ulbrich-Piloty filter. In the plot the output of the filter is corrected for gain loss and offset. In this way a maximum gray level (255 quantisation steps) of a pixel in the CCD signal will have a correspondig filter output with a maximum gray level of 255 quantisation steps also. As shown in the figure, this filter type preserves the step like pixel information in the CCD-signal almost completely. The output of the filter is delayed for about two pixel periods. The delay is caused by the group delay of the low-pass filter. This causes no extra artefacts in the re-sampling process since the image is shifted only slightly and no extra loss of image information is introduced. If the effects may become disturbing, it can be suppressed by introducing the same delay in the sample moments at the re-sampling stage.



ooo : response of combination of a Bessel filter and a Notch filter  
 .-. : response of an Ulbrich Piloty low-pass filter.

Figure 23. Responses to step-like pixel information. (corrected for gain loss and offset in the graylevel)

**The combination of a second order Notch filter and a 4th order Bessel low-pass filter** causes less attenuation in the pass band than the Ulbrich-Piloty filter, but has a phase characteristic that is not as linear. The amplitude and phase behaviour of the filter combination are shown in figure 24. In this figure the filter combination was designed for a CCD-pixel-frequency of 10 MHz.

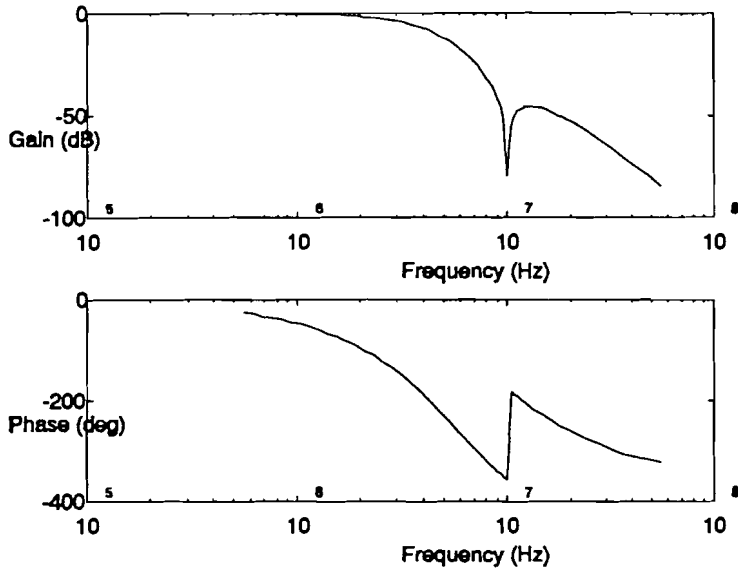


Figure 24. Amplitude and phase characteristics of the combination of a Notch filter and a fourth order Bessel low-pass filter simulated in MATLAB.

A simulation of the transient response by a filter combination containing a Notch filter and a Bessel low-pass filter is also plotted in figure 23. As can be seen in this figure, the preservation of step-like information is almost equal for both filter types, although the Ulbrich Piloty filter adds some more delay.

The Notch filter is a second order band reject filter with a zero in the transfer function at the pixel frequency ( $\omega_p/(2\pi)$ ). The transfer function of the Notch filter is defined as follows:

$$H(s) = \frac{1 + \left(\frac{s}{\omega_0}\right)^2}{1 + s\frac{2\zeta}{\omega_0} + \left(\frac{s}{\omega_0}\right)^2}$$

17.

For the applied filter the parameter  $\zeta$  is set to 1. The applied Bessel filter is a fourth order low-pass filter with its cutoff frequency located at the Nyquist frequency.

Next to simulating step like pixel information so called 'sweep' signals are also used for the simulation of transient responses. A sweep signal is shown in figure 25A. This signal has a spatial frequency that increases, moving along the x-axis. In figure 25B the simulation results of the corresponding CCD output signal are shown. The transient responses of the two filter types to this CCD output signal are shown in figure 25C. Here the solid line represents the Ulbrich-Piloty filter response and the dotted line represents the response of the Bessel\_Notch filter combination.

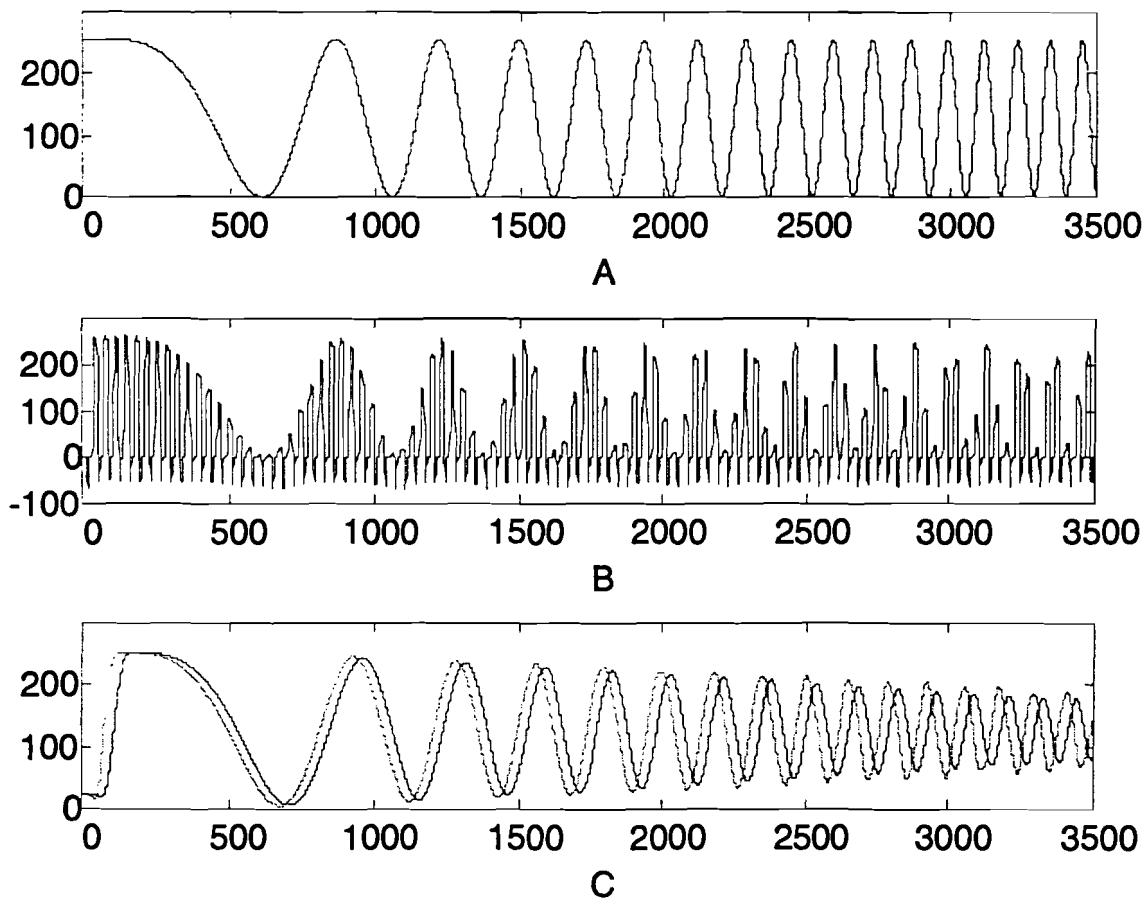


Figure 25. A: Pixel information, B: CCD-output signal, C: Filter responses.

Here, the simulation of the CCD signal consists of 100 pixel periods. Each pixel-period in the CCD output signal is represented with 35 datapoints. A detail of figure 25C is shown in the following figure. It shows that an Ulbrich Piloty low-pass filter has a transient response to a sweep signal that is somewhat more monotonic than the Bessel-Notch filter combination.



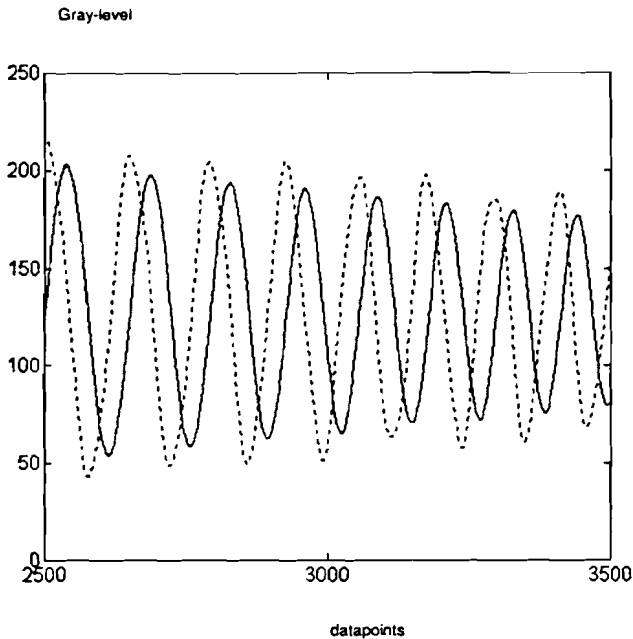


Figure 26. Close-up of the filter responses in figure 25C.

Both the Ulbrich Piloty filter and the combination of a Notch filter and a Bessel low-pass filter can be applied as a time-continuous interpolation filter. Each of these two filter types has its advantages and disadvantages. For example, the Ulbrich-Piloty filter has better phase characteristics than the combination Notch-Bessel. On the other hand, the combination of a Notch filter and a Bessel filter causes less attenuation of frequencies below the Nyquist frequency than the Ulbrich Piloty filter. The performance of the combination of a Notch filter and a Bessel low-pass filter highly depends on the exact location of the rejection-band of a Notch filter. Because of component variations or tolerances, the design of a band-reject (Notch) filter-structure having a zero in the transfer function at the clock frequency of several MHz, must be performed carefully. An Ulbrich-Piloty low-pass filter is less sensitive to component tolerances and therefore a filter of this type has been implemented for practical tests.

It could be possible that other pre-cautions like a maximally flat passband are found to be more important than for example retaining step-like information or the attenuation of frequency components that are above the Nyquist frequency. In that case, a new filter characteristic, that optimally combines the pre-cautions, must be found. Designing such filters is beyond the scope of this report.

## 5. Implementation

The simulations that were performed with SIMULINK, used a transfer function in the Laplace domain to describe the filter properties. The filter is chosen to be designed with discrete components. For actual implementation, the values of the different inductors and capacitors must be calculated. One can choose several network configurations in order to realise a filter having the desired transfer function. Often a filter network is designed in a so called ladder structure. A ladder network consists of a sequence of alternating series and shunt branches. In the case of lossless transmission networks the branches are composed of one or several reactive elements (capacitors and inductors). Designing filters as lossless transmission networks in an LC-ladder structure has the following advantages:

- Ladder filters offer a good stability in the stopband because attenuation poles are produced by resonance circuits that can be built of high quality passive components.
- LC filters have excellent linearity.
- If properly designed, these networks have a good stability in the passband.
- A ladder filter composed of reactive elements (L,C) generates no extra noise in the output signals.
- Compared to active filters, LC filters have an unequalled dynamic range.
- The passive filters need no power supply and have no dissipation.
- In active filters, for example biquad filters, each conjugated pole-pair is generated independently and such filters are therefore more sensitive to component variations than an LC-filter.
- A disadvantage of a lossless LC-ladder structure is the fact that frequencies within the passband are attenuated with a constant factor. If the source-impedance and the load-impedance are equal this attenuation factor is 2.

Because of the several advantages the Ulbrich-Piloty filter is designed in a passive LC-ladder structure.

### 5.1. Ladder network decomposition

The design of an LC-ladder network [2] is based on the idea that for a lossless transmission network, the transmitted power into a load resistor is equal to the reference power minus the reflected power.

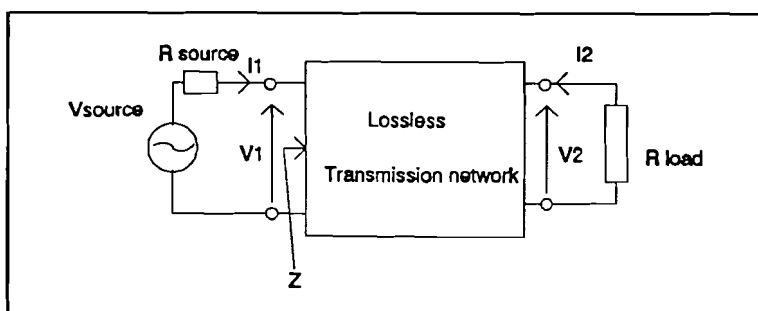


Figure 27. A lossless transmission network, placed between a source and a load resistor.

In figure 27, the reference power ( $P_{ref}$ ) is equal to  $V_1 \cdot I_1$ . The transmitted power ( $P_t$ ) is equal to  $V_2 \cdot I_2$ . Here, the maximally available power of the source is equal to  $P_{ref}$ . In the case of a matched generator,  $R_{source}$  is equal to  $R_{load}$ . The maximal power transfer is achieved if  $V_1 = V_2$  and  $I_1 = I_2$ . In that case the reference power is equal to:

$$P_{ref\ max} = \frac{|V_{source}|^2}{4R} \quad 18.$$

With  $Z$  being the input impedance of the lossless transmission network, terminated with a load resistor, the reflection coefficient  $\rho$  is equal to:

$$\rho = \frac{Z - R}{Z + R} = \text{reflection coefficient} \quad 19.$$

The reflected power  $P_r$  and the transmitted power  $P_t$  are then defined as:

$$\begin{aligned} P_r &= P_{ref} |\rho|^2 \\ P_t &= P_{ref} - P_r = P_{ref} [1 - |\rho|^2] \end{aligned} \quad 20.$$

In the Laplace domain, the normalised input impedance and the reflection coefficient can be defined as:

$$z(s) = \frac{Z(s)}{R} = \text{normalised input impedance} \quad 21.$$

$$\rho(s) = \frac{Z(s) - R}{Z(s) + R} = \frac{z(s) - 1}{z(s) + 1} = \frac{F(s)}{E(s)} \quad 22.$$

The normalised input impedance can also be expressed as:

$$z(s) = \frac{E(s) - F(s)}{E(s) + F(s)} \quad 23.$$

The polynomials  $E(s)$ ,  $P(s)$  and  $F(s)$  are not independent to each other, but are connected by the equation:

$$E(s)E(-s) = F(s)F(-s) + P(s)P(-s) \quad 24.$$

The power transfer function ( $P_t / P_{ref}$ ) can then be expressed as:

$$\begin{aligned}
\frac{P_t}{P_{ref}} &= 1 - |\rho(s)|^2_{s=j\omega} = 1 - \left| \frac{F(s)}{E(s)} \right|^2_{s=j\omega} \\
&= \left| \frac{E(s)E(-s) - F(s)F(-s)}{E(s)E(-s)} \right|^2_{s=j\omega} \\
&= \left| \frac{P(s)P(-s)}{E(s)E(-s)} \right|^2_{s=j\omega}
\end{aligned}$$

25.

Now the transfer function T(s) can be described as follows:

$$T(s) = \frac{V_2}{V_1} = \frac{P(s)}{E(s)}$$

26.

For the low-pass filter types that are described in 4.3. only their transfer function T(s) is known. In order to decompose this transfer function into a ladder network, one can calculate the corresponding normalised input impedance using the formulas described above.

For this purpose a so called script file (called 'ladder.m') in MATLAB is written. Given the set of polynomials P(s) and E(s), the script file first calculates the product F(s)F(-s) using the formula F(s)F(-s)=E(s)E(-s)-P(s)P(-s). The product F(s)F(-s) is a polynomial function containing only even powers of s and can be written as:

$$\begin{aligned}
F(s) &= K(s-n_1)(s-n_2) \dots (s-n_i) \\
F(s)F(-s) &= K^2(s-n_1)(-s-n_1)(s-n_2)(-s-n_2) \dots (s-n_i)(-s-n_i) \\
&= K^2(s^2+n_1^2)(s^2+n_2^2) \dots (s^2+n_i^2)
\end{aligned}$$

27.

, with K being a constant factor and n<sub>1</sub> to n<sub>i</sub> being the roots of the function F(s).

- At this stage, the polynomial function F(s) is not yet known, and it must be derived from this product. In the s-plane, the roots of the product F(s)F(-s) can generally be divided into four different types (as shown in figure 30) :

- 1- Roots that are located at the origin. These roots are present in combined pairs at the origin.
- 2- Roots on the real axis. These roots are present as combined pairs that are mirrors of each other with respect to the imaginary axis.
- 3- Roots located on the imaginary axis. Roots of this type appear as combined pairs of double-roots that are mirrors of each other with respect to the real axis.
4. Roots that are not of type 1, 2 or 3. Roots of type 4 appear in groups of four that are mirrors of each other with respect to the imaginary and real axis.

In figure 28 one example of each of these four types is shown.

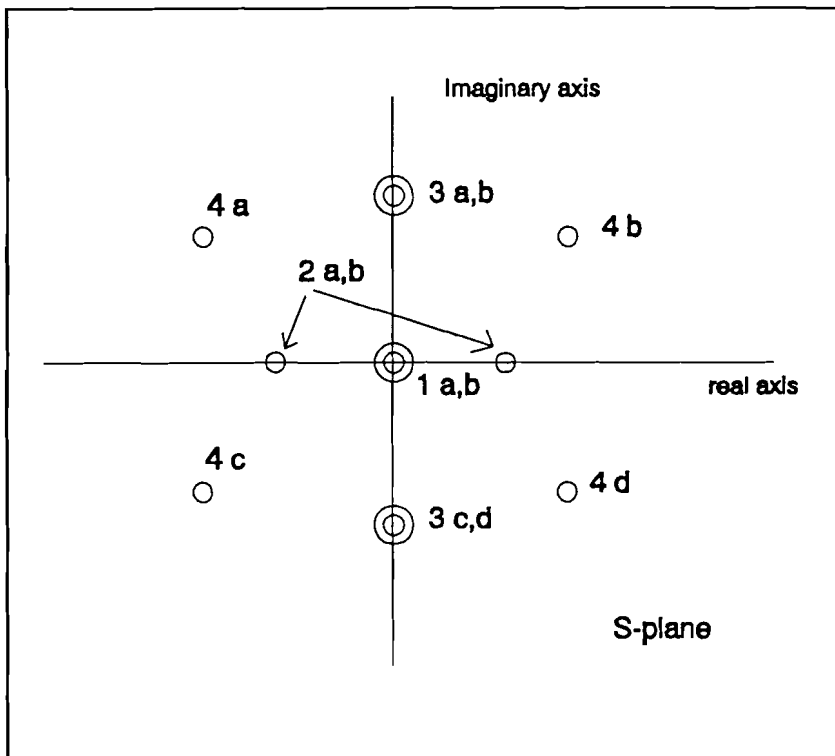


Figure 28. Four types of roots of the product  $[F(s)F(-s)]$ .

The MATLAB script file 'ladder.m' checks and classifies the roots of the product  $F(s)F(-s)$ . Then the polynomial  $F(s)$  is composed as follows:

- Of each pair of roots of type 1, one root becomes a root of the polynomial  $F(s)$ .
- Of each pair of roots of type 2, one root becomes root of  $F(s)$
- Of each group of four roots of type 3, one mirrored pair becomes a pair of roots of  $F(s)$ .
- Out of each group of four roots, one mirrored pair with respect to the real axis becomes a pair of roots of  $F(s)$ .

In the case of roots of type 2 or 4, one can choose to roots in the right half of the s-plane or the roots in the left half of the s-plane to compose  $F(s)$ . The script file 'ladder.m' chooses the roots of the left half of the s-plane for the composition of  $F(s)$ . For the example in figure 30, the polynomial  $F(s)$  would be composed from the roots  $1a$ ,  $2a$ ,  $3a+c$  and  $4a+c$ .

At this stage, the polynomial  $F(s)$  is known and the normalised input impedance  $z(s)$  can be calculated, using the polynomials  $E(s)$  and  $F(s)$ . The input impedance  $z(s)$  has a numerator polynomial and a denominator polynomial.

In order to calculate the values of the components in the ladder network with this input impedance the script file 'ladder.m' rewrites the function of the normalised input impedance as follows:

$$\begin{aligned}
z(s) &= \frac{E(s) - F(s)}{E(s) + F(s)} = \\
&= \frac{a_i s^i + a_{i-1} s^{i-1} + \dots + a_0}{b_i s^i + b_{i-1} s^{i-1} + \dots + b_0} = \\
&= z_1 + \frac{1}{y_2 + \frac{1}{z_3 + \frac{1}{y_4 + \frac{1}{z_5 + \frac{1}{y_6 + \dots + \frac{1}{z_i + R}}}}}
\end{aligned}$$

with  $R=1$  (normalised load impedance)

28.

Writing the impedance function this way is generally called 'Ladder Decomposition'. Here  $Z_i$  represents a complex impedance and  $Y_i$  represent a complex conductance. The output of the script file consists of the polynomials describing impedances  $Z_i$  and the conductances  $Y_i$ .

In the next figure the topological layout of this ladder decomposition is shown.

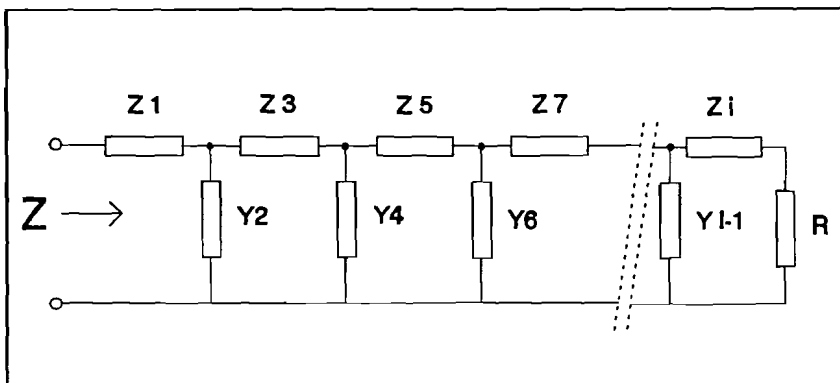


Figure 29. Impedances and conductances in a ladder network.

Generally, the transfer function  $T(s)$  is designed with respect to a normalised bandwidth and a normalised load impedance. The resulting values of  $Z_i$  and  $Y_i$ , have to be denormalised in order to find the actual values of the components of a filter having the desired bandwidth and load impedance.

The first step is the frequency denormalisation, resulting in a bandwidth of  $\omega = \omega_0 = 2\pi f$ . With a normalised frequency variable  $\Omega$ , the bandwidth of the normalised ladder network is  $\Omega_0 = 1$  rad/sec. Frequency denormalisation can then be performed using the transformation:

$$\Omega = \frac{\Omega_0}{\omega_0} \omega$$

29.

This transforms a capacitance  $C$  into  $C'$  and an inductance  $L$  into an  $L'$  through:

$$C' = \frac{\Omega_0}{\omega_0} C$$

$$L' = \frac{\Omega_0}{\omega_0} L$$

30.

The next step is impedance denormalisation. The load impedance R is transformed into R'. The inductances and capacitances are then denormalised as follows:

$$L'' = \frac{R'}{R} L'$$

$$C'' = \frac{R}{R'} C'$$

31.

After calculating the denormalised values of all inductances and capacitances in the network, the properties of the desired filter network are known.

## 5.2. Pspice network-analysis

For a realistic simulation of the filter behaviour, the network simulation software Pspice is used. First, the values of the filter components are calculated as described in paragraph 5.1 and a schematic network structure is made for Pspice. For the simulations, the Ulbrich-Piloty filter, as described in chapter 4, is designed for a CCD-signal with a pixel frequency of 14.175 MHz. Both the source impedance and the load impedance are set to 50 Ohm. The component values that are calculated for this filter are shown in the following schematic:

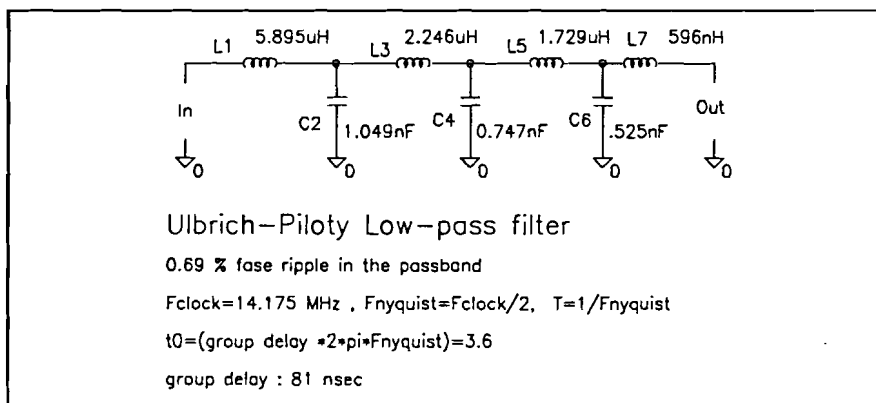


Figure 30. Schematic of the Ulbrich-Piloty low-pass filter with ideal components.

In principle, these component values can be approximated with all tunable coils and tunable capacitors. However, this implies much tuning effort for each filter that will be build. One can also approximate the component values using standard components of the E-12 or the E-6 series for coils and capacitors. This implies that the transfer function of the filter will be slightly altered. A filter has been implemented with coils and capacitors of the E-12 series and is shown in figure 31.

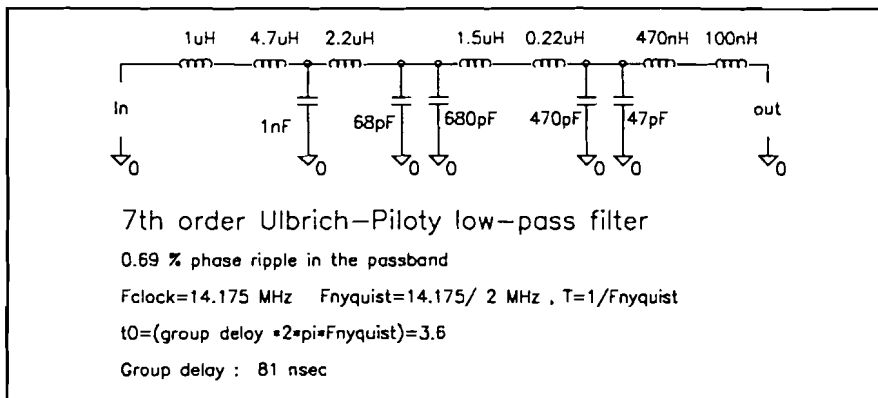


Figure 31. Schematic of the Ulbrich Piloty low-pass filter with components of the E-12 series.

In addition to the non-ideal values of the coils and capacitors, the components of the E-12 series have a tolerancy of 10%. In order to evaluate the influences of non-ideal component values, so called 'Monte Carlo runs' are performed in Pspice. A set of Monte Carlo runs comes down to arbitrary varying the component values within their given tolerances, and simulating the resulting filter behaviour in the time- or frequency-domain. In this way, for example a set of Bode plots can be drawn in one figure, giving an indication of the sensitivity of the tranfer function to non-ideal component values.

In figure 32, Monte Carlo runs for the Ulbrich-Piloty filter in the frequency domain are shown. Here, 10 Monte Carlo runs are performed with coils and capacitors having a tolerance of 10 %. As can be seen in the figure, the attenuation at the Nyquist frequency (7.0875 MHz) can vary from approximately 14 dB to 17 dB. At the clock-frequency (14.175 MHz) the attenuation can vary from 61 dB to 65 dB.

A set of Monte Carlo runs for the transient response to step like pixel information are shown in figure 33. It shows that, due to component values having tolerances of 10 %, some overshoot or undershoot can occur. These overshoots or undershoots are in the order of 3 %. Ringing effects are negligible.



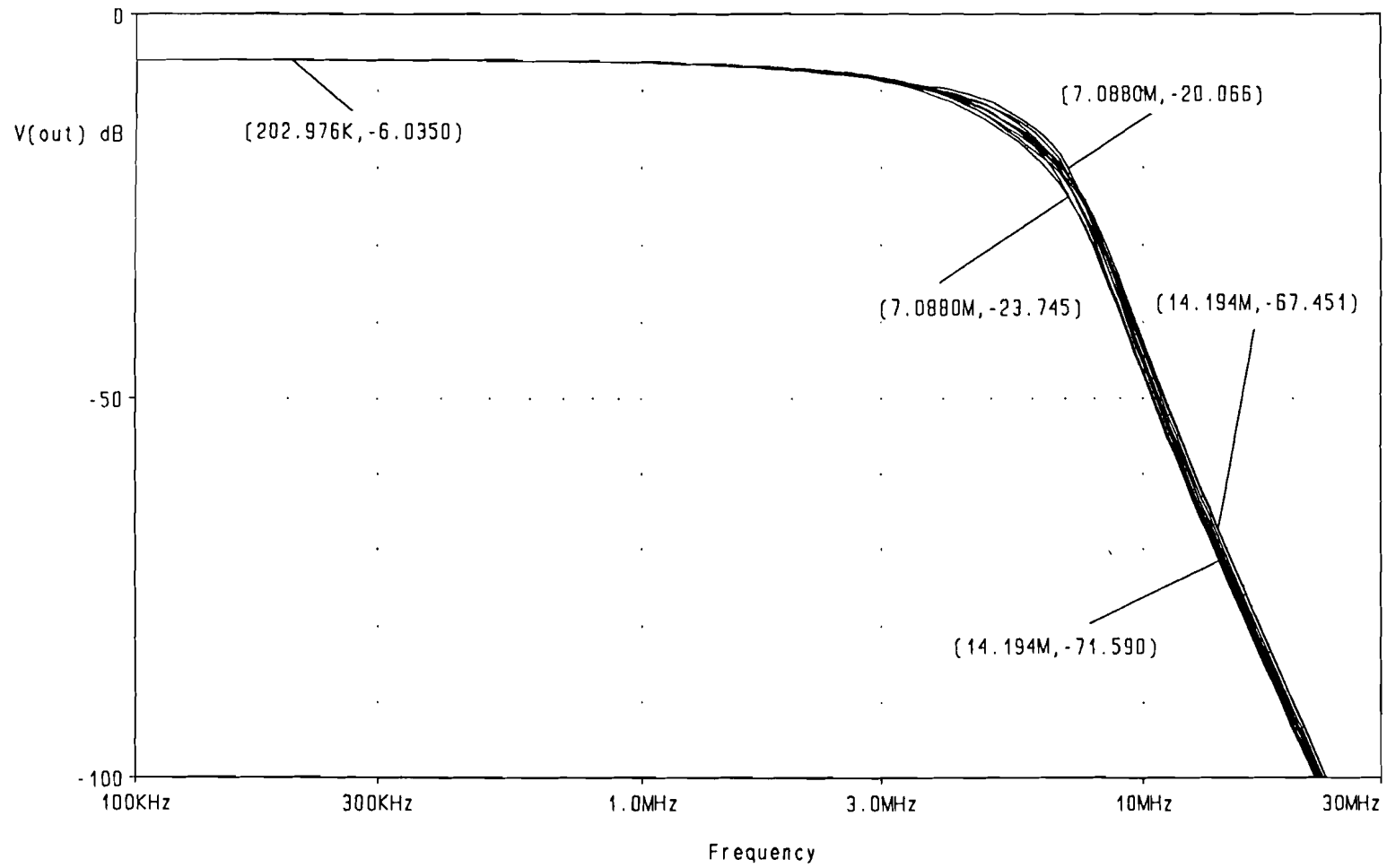


Figure 32. Monte Carlo analysis in the frequency domain

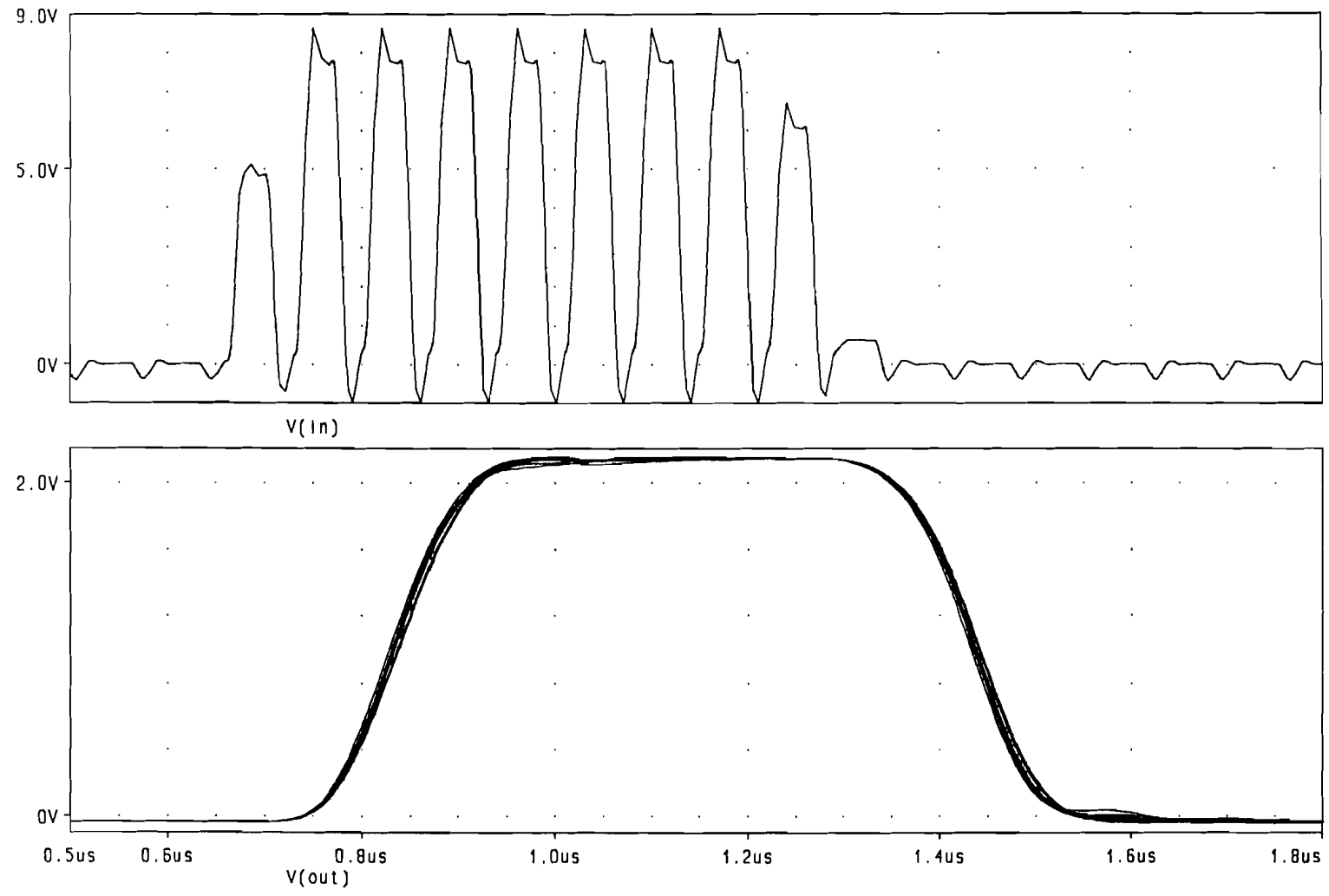


Figure 33. Transient Monte Carlo analysis

## 6. Tests

IN order to test the practical performance of the Ulbrich-Piloty filter, several tests are performed. The filter characteristics in the frequency domain are measured and some scans are made using the low-pass filter to filter the block-pulsed CCD signal.

### 6.1. Frequency sweep

The frequency behaviour of the implemented Ulbrich-Piloty filter is tested by generating a series of frequencies with a programmable signal generator and measuring the amplitude-response of the filter. The results of this test are shown in figure 34.

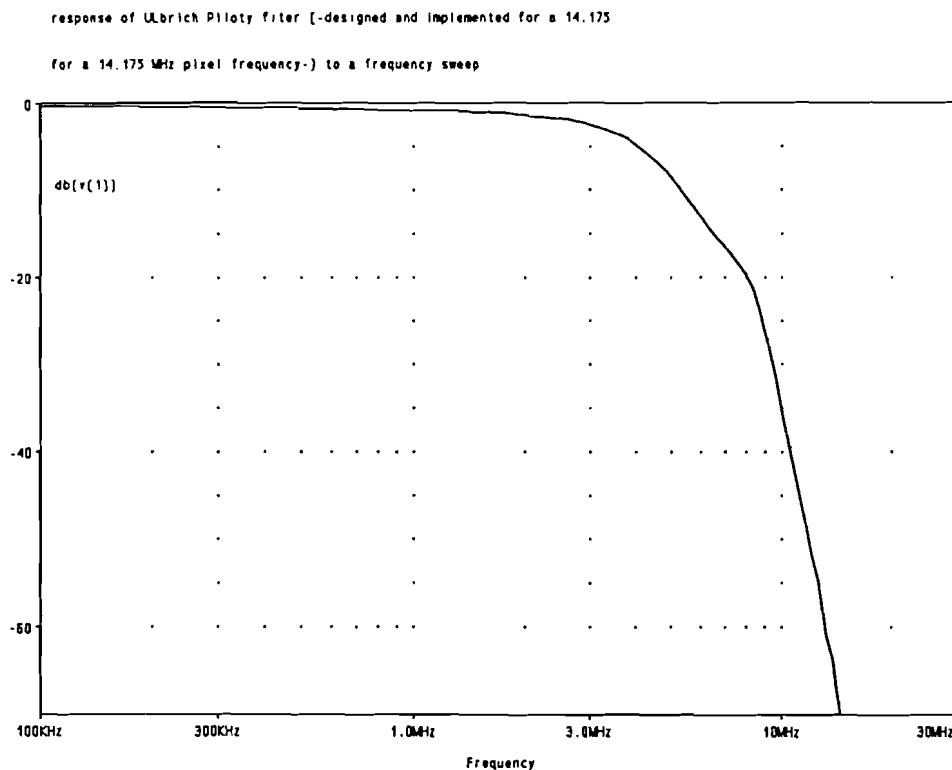


Figure 34. Frequency response of the implemented Ulbrich-Piloty filter.

The measured attenuation of the filter at the Nyquist frequency (7.0875 MHz) and at the pixel frequency (14.175 MHz) is approximately 16.8 dB and 67 dB respectively. The frequency characteristics are within the range as predicted by the Monte Carlo analysis in paragraph 5.2.

### 6.2. Test scans

The performance of the Ulbrich-Piloty low-pass filter in an actual scanner is tested by performing some test scans. The test scans are made using a scanner with an addressability of 125 dpi. Two scans of an original image, containing text information, are made. First, the image is scanned without making use of the filter. Next, the image is scanned using the filter at the output of the CCD-sensor. The results of these scans are shown in figure 35A and B.

<b>Incorporated</b>			<b>Incorporated</b>		
uartered in San Jose, California ndustrial and high-technology rketing, planning, purchasing est's major service areas cover s, office systems, electronic p uring automation, and semic alifornia headquarters, Dataqu			uartered in San Jose, California ndustrial and high-technology rketing, planning, purchasing est's major service areas cover s, office systems, electronic p uring automation, and semic alifornia headquarters, Dataqu		
<b>STANDA</b>			<b>STANDA</b>		
Standard		ISO standard	Standard		ISO standard
Size			Size		
	Inches	Designation		Inches	Designation
1575	34 x 45	A0	1575	34 x 45	A0
889	23 x 35	A1	889	23 x 35	A1

Figure 35A. Scan of a text-original without low-pass filtering the CCD-signals. B. Scan of a text-original with low-pass filtered CCD-signals.

Unfortunately, the printer has a major effect on the image quality of the images shown in this report. Nevertheless, this test shows that the text-image, scanned using an Ulbrich Piloty low-pass filter as interpolation filter, is more smoothed in the horizontal direction than the non-filtered text-image. This was to be expected as the low-pass filter attenuates frequencies below the Nyquist frequency. An example of the smoothing of the image information can be found by comparing the words 'Designation' at the bottom-right in both figures 35A and 35B.



Horizontal direction:

Nyquist frequency

Sample frequency

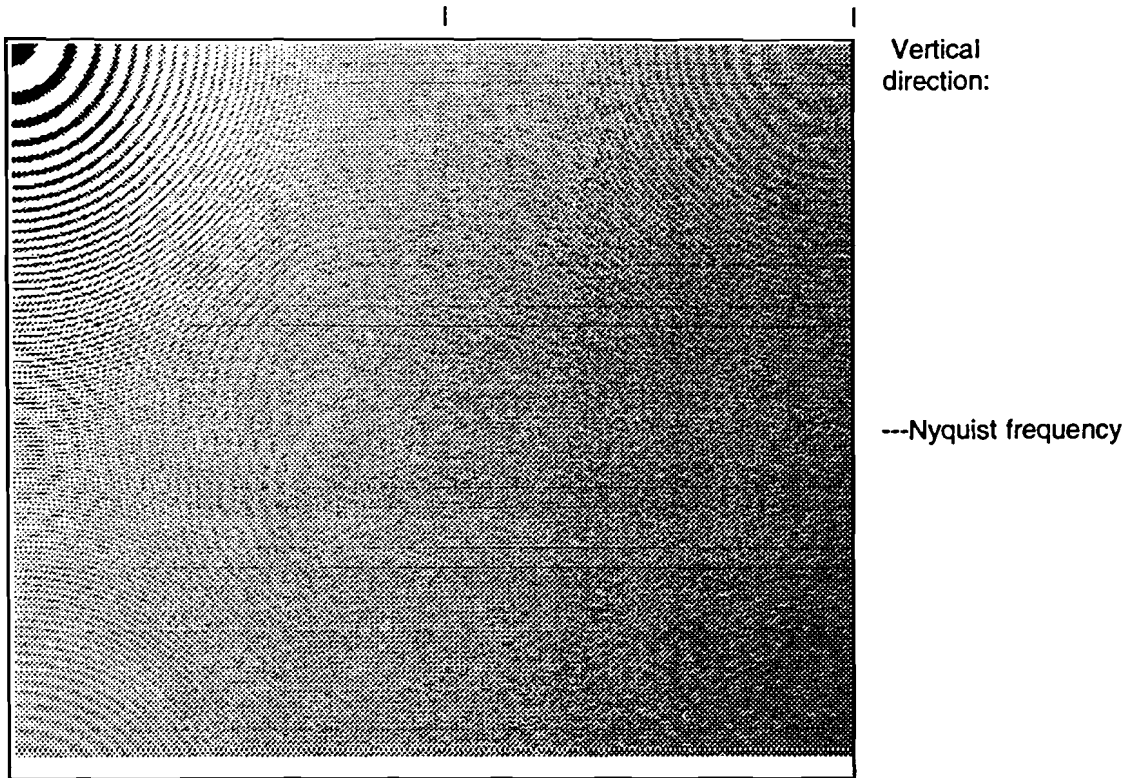


Figure 37. Test chart scanned with low-pass filtered CCD-output-signals

When comparing the corresponding 2-dimensional images shown in figures 38 and 39, the image that is smoothed by the low-pass filter is hardly distinguishable from the non-filtered image. The Moiré patterns at the Nyquist frequency in the horizontal direction and along the diagonal, are attenuated due to the low-pass filtering. The frequency components in the image at the sample frequency are 'folded back' or aliased to low-frequency patterns due to the optical sample process and cannot be filtered by the low-pass filter. Therefore, the Moiré patterns due to these low-frequencies are visible in both the filtered and the non-filtered scan of the test-chart.

In order to compare the results of these scans, without the disturbing printer characteristics, both the horizontal line and the vertical line that cross the center of the circles are extracted and plotted in the figures 38 and 39. The vertical axes in the plots represent the gray level and the horizontal axes represent the distance from the center of the circle pattern (measured in numbers of pixels). The figures 38 A and 38 B clearly show the attenuation of frequencies below the Nyquist frequency by the filter.

The spatial frequencies in the vertical direction are not affected by the low-pass filter. This can be seen in the envelopes of the plots in the figures 39A and 39B that are almost equal. The major difference between both plots is located approximately between pixel-numbers 170 to 190. At this location, the spatial frequency of the original image is about the Nyquist frequency. In the case of sampling these spatial frequencies, phase effects can become relatively large. The average gray level of the pixels is then dominated by the phase difference between the pixel locations and the spatial information. When performing the scans of the test-chart, this test-chart was slightly moved after scanning without a low-pass filter and before scanning with low-pass filtered CCD-signals. This movement caused a different phase effect.

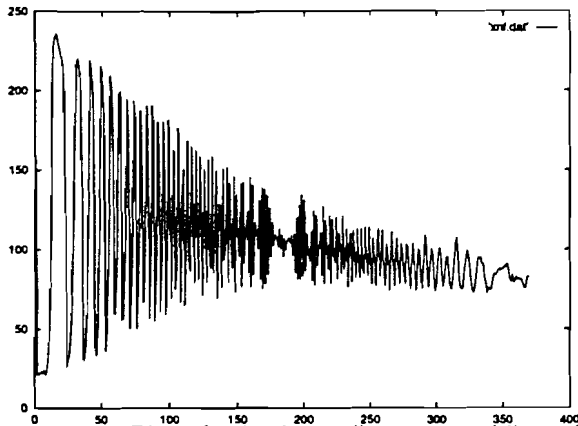
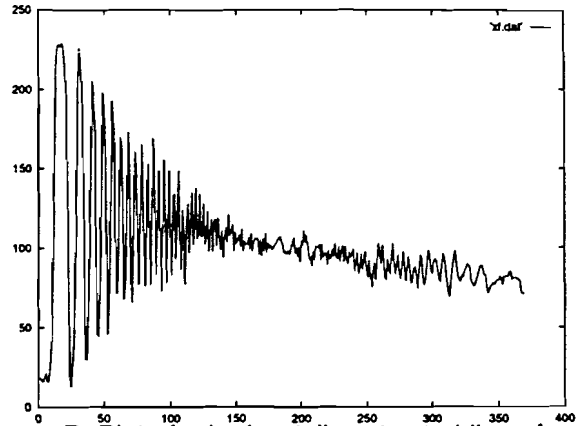


Figure 38A. Plot of a horizontally extracted line of the test-scan (figure 36) without low-pass filtering.



B. Plot of a horizontally extracted line of the test-scan (figure 37) with low-pass filtering

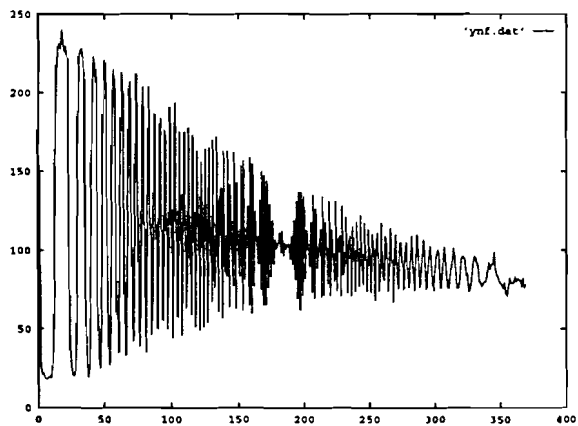
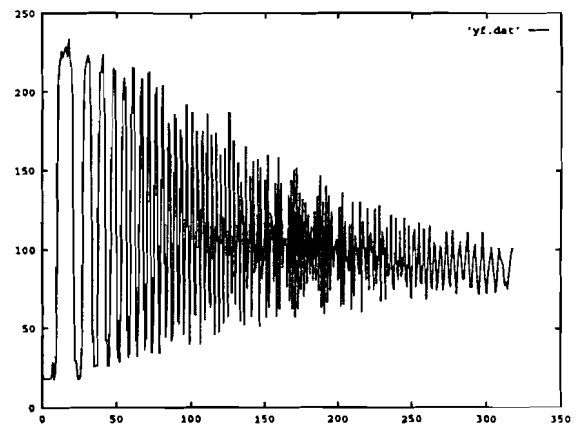


Figure 39 A. Plot of a vertically extracted line of the test-scan (figure 36) without low-pass filtering the CCD signals.



B. Plot of a vertically extracted line of the test scan (figure 37) with low-pass filtering the CCD signals.

In the figures 38 and 39 the Nyquist is located at approximately pixel-number 180.

## 6.2. Noise reduction

One of the additional advantages of time-continuous low-pass filtering is the attenuation of high frequency noise in the CCD signal. It is difficult to estimate the power of the noise components in this signal since there are several different noise sources in the process-path from spatial sampling by the CCD sensor to quantisation and storage of the picture information.

In figure 40, a schematic overview of these noise sources in the scanning process is shown.

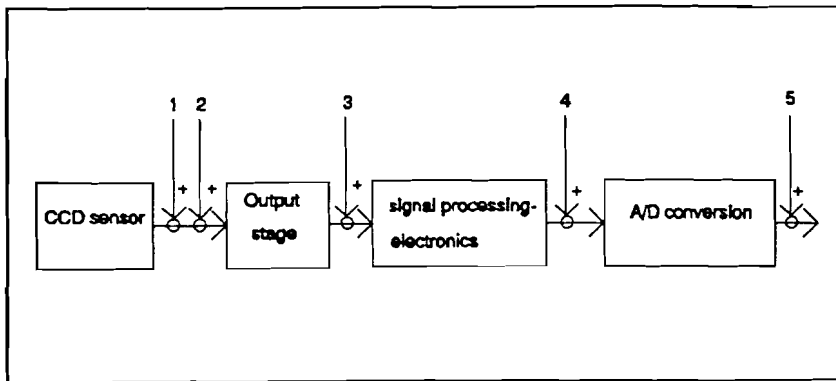


Figure 40. Five different noise sources in the scanning process.

In the CCD sensor, pixel noise (1) is generated by non-ideal charge transfer of pixel information. This noise component is indistinguishable from pixel information and therefore it cannot be filtered in the output signal of the CCD sensor. The pixel to pixel noise (2), which can be seen as a form of offset variation, is caused by variations in the floating diode voltage level. This noise source is generally low-frequent and can be reduced by using Correlated Double Sampling techniques. Correlated double sampling is achieved by sampling both the amplitude of the pixel pulse and the voltage level in the corresponding floating diode period. By subtracting these samples, the offset variations can be effectively reduced.

The output gate of the CCD sensor generates broadband noise (3). Although one cannot easily estimate the form of the power spectrum of this noise source, frequency components that are higher than the pixel frequency, can be seen in the CCD signal.

The signal processing electronics that are connected to the CCD-sensor, add little noise to the output signal (4). By choosing high quality components, this noise-addition can be kept so small that it plays no role of importance.

Quantisation noise is generated by the A/D converter (5). The quantisation noise is set by the number of quantisation steps and can therefore only be decreased by implementing an A/D converter with more quantisation steps.

The high frequency noise components in the output signal of the signal processing electronics will be filtered by the smoothing- or interpolation-filter. The reduction of high frequent noise by the Ulbrich-Piloty interpolation filter, designed for CCD-sensors with a pixel frequency of 14.175 MHz, is measured as follows: The input of the filter is connected to a waveform generator that simulates white noise in the frequency band from 0 to 125 MHz. The noise power at the output of the filter is then measured and compared with the noise power at the input. The noise amplitude at the input was set to 155 mV (R.M.S. value) The measured noise amplitude at the output of the Ulbrich Piloty filter was 27 mV (R.M.S. value). So, for this test-case, the input noise is reduced:  $20 \cdot \log(5.7) \approx 15$  dB.

Since the noise in CCD signals can vary from CCD-sensor to CCD-sensor and depends on the quality of several components and parts in the scanning process, the measured noise reduction by the Ulbrich-Piloty filter is only an indication of the high frequency noise attenuation that can be achieved by such filters. The improvement of the signal to noise ratio for CCD signals distorted with white noise can roughly be approximated as follows:

The noise in the input signal is experimentally found to be bandlimited to approximately 4 times the pixel frequency of the CCD sensor. For simplicity, the filter is supposed to be an ideal low-pass filter that is bandlimited to the Nyquist frequency (half the pixel frequency). Suppose the pixel pulses in the CCD-output are set to a duty-cycle of 50 %. In that case, the filtered output voltage that repre-



sents the pixel information, is approximately half the voltage of the non-filtered pixel amplitude. In the power-spectrum these pre-assumptions imply the following:

$$P_n = B\eta = 4 F_{pixel}\eta = 4 * 2 * F_{Nyquist}\eta$$

$$P_{nf} = \frac{1}{2} F_{pixel}\eta = F_{Nyquist}\eta$$

$$\begin{aligned} \text{Reduction of Noise power} &= 10 \log \left( \frac{P_n}{P_{nf}} \right) \\ &= 10 \log (8) = 9 \text{ dB} \end{aligned}$$

$$\begin{aligned} \text{Reduction of signal power} &= 10 \log \left( \frac{V_i^2}{V_o^2} \right) = \\ &= 20 \log \left( \frac{V_i}{V_i * 0.5} \right) = 20 \log (2) = 6 \text{ dB} \end{aligned}$$

Here  $P_n$  and  $P_{nf}$  represent the noise power and the noise power after low-pass filtering respectively. The bandwidth of the noise spectrum is represented by  $B$  and the noise power per Hz is represented by  $\eta$ . In this case, the signal to noise ratio is improved with  $(9 \text{ dB} - 6 \text{ dB}) = 3 \text{ dB}$ , which comes down to a factor 2.

## 8. Conclusions

The application of time-continuous analogue filters for interpolation of CCD-signals has several advantages. A major advantage is that it offers the possibility of re-sampling the smoothed signals at arbitrary sample frequencies, making it easy to zoom in or out. The extra memory that is often needed for digital interpolation algorithms is not needed here. Also high frequent noise in the output signals of CCD-sensors is attenuated, which increases signal to noise ratio. Using the filter, the exact sample-moments in the analogue-to-digital converter are less critical than sampling the non-filtered, blockpulsed, CCD signal.

A filter that optimally combines the pre-cautions like effective attenuation of frequencies that are higher than the Nyquist frequency and retaining an almost linear phase characteristic, is the Ulbrich-Piloty low-pass filter. It has been designed in a simple structure and can be built with low-cost inductances and capacitances. The Ulbrich-Piloty low-pass filter has been implemented and tested. Practical results have proven that time-continuous analogue filtering is a usefull technique and can be applied as an alternative for conventional interpolation techniques like digital interpolation or time-discrete interpolation by switched capacitor filters.

The analogue low-pass filter unfortunately causes some attenuation at frequencies that are lower than the Nyquist frequency, decreasing the sharpness of scanned images. Instead of this filter, also a combination of a Bessel low-pass filter and a Notch filter could be applied as time-continuous analogue interpolation filter. In this case there is less attenuation in the passband. On the other hand, this filter has a phase characteristic that is less linear and is more sensitive to component variations or tolerances. This filter-combination has not yet been implemented and tested in practice.

It could be that other filters will have a better performance if pre-cautions like for example a maximally flat passband are found to be much more important than for example retaining step-like information. In that case, a new optimal filter characteristic has to be found, which is beyond the scope of this report.

## 7. Recommendations

\* The analogue smoothing filters attenuate high frequent noise components in the CCD signals. Low frequent noise components are not attenuated and can cause low frequent variations in the filtered output signals. These offset variations in CCD-signals may be attenuated by using Correlated Double Sampling (CDS) techniques. Here both the pixel amplitude and the voltage of the corresponding floating-diode-period are sampled. By subtracting these two samples from each other, the low frequent variations, due to noise, can be corrected. A comparable sort of correlated double sampling could be applied in combination with the analogue interpolation filter. This is shown in figure 41.

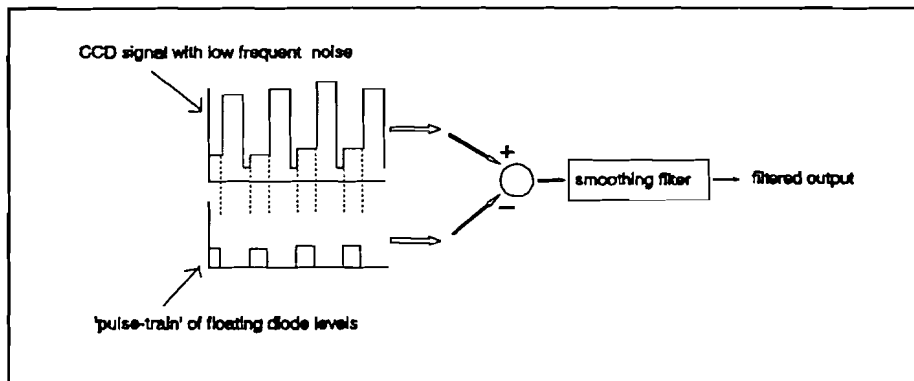


Figure 41. Reduction of Low frequent noise in CCD signals.

In this case, a pulse train with pulse amplitudes that are modulated by the floating diode periods must be created. Low frequent offset variations can be partly attenuated by subtracting the pulse-train with a certain factor from the CCD-signal followed by filtering the resulting signal with the analogue interpolation filter. In comparison with correlated double sampling, one can call this method 'Correlated Double Filtering'. Great care must be taken when choosing the right subtraction factor. If not chosen carefully, correlated double filtering could introduce extra noise components.

\* The Ulbrich-Piloty filters has some attenuation of frequencies below the Nyquist frequency. Some correction to this can be made by adding a lead filter (amplifying higher frequencies) in cascade with the smoothing filter. However, in order to preserve for example step-like information, this lead filter should be designed with a phase characteristic that is almost linear, which may be a problem.

\* Another sharpening filter that intensifies step-like information takes the sum of the smoothed CCD-signal and the absolute value of its second order derivative of this smoothed CCD signal. This operation causes step like information to be sharpened. More detailed information can be found in [13].

## References

- [1] "The CCD Image Sensor"  
Brochure Thomson Composants Militaires et Spatiaux  
Dec. 1990
- [2] E. Christian,  
'LC-Filters, Design, Manufacturing and Testing'  
Wiley Series on Filters, 1983
- [3] McCurnin, T.W. et al.  
'Charge coupled device signal processing models and comparisons',  
Journal of Electronic Imaging 2(2), p. 100-107 (april 1993)
- [4] B. Heck, J. Speidel  
'A Method for the implementation of high speed digital filters for  
video signals'  
Signal Processing III: Theories and applications p.207-210  
Elsevier Science Publishers 1985
- [5] H.Khorambadi et al.  
'High frequency CMOS continuous time filters'  
IEE Journ. Solid State Circuits, Vol. SC-19 p.939-948
- [6] L.Levi,  
'Applied Optics, a guide to Optical System Design'  
J. Wiley & Sons, New York, Vol.2. 1980
- [7] B. Lux et al.  
'Die Kantendarstellung verbessern,  
Neues Schaltungskonzept wertet CCD-Zeilen-Signale aus'  
Elektronik 18/31.8.1990 Vol. 39 p. 112-116
- [8] J.Ritzerfeld, H.Hegt, P. Sommen, H. van der Meer,  
"Realisering van Digitale Signaalbewerkende Systemen",  
Januari 1993, Faculteit Elektrotechniek,  
Technische Universiteit Eindhoven, Dictaat nr.5750
- [9] C.de Rooij,  
"Analoog Digitaal Conversie"  
1985, Faculteit Elektrotechniek,  
Technische Universiteit Twente
- [10] Schreiber W.F.  
"Fundamentals of Electronic Imaging Systems",  
Some aspects of image processing  
Springer Verlag, 1991, Editor: Huang T.S.
- [11] Schreiber W.F.  
"Transformation between Continuous and Discrete Representations of  
Images : A Perceptual Approach."  
IEEE Trans. on pattern analysis and Machine Intelligence,  
Vol. PAMI-7 No.2. March 1985

- [12] J.Speidel, B.Heck  
'The design and implementation of digital filters for pre- and postfiltering and sampling rate conversion of video signals.'  
IEE 2nd international conference on Image Processing nr.265 (1986)  
p.210-214
- [13] R. van Weezel,  
'Video Handboek'  
De Muiderkring, Bussum  
1977.



FORMULIER MANAGEMENT SUMMARY  
stageverslagen / -rapporten

Korte samenvatting van het verslag / rapport:

CCD sensoren in scanners bemonsteren het beeld van een origineel document en bieden deze informatie in de vorm van een puls-amplitude gemoduleerd uitgangssignaal aan. De informatie dichtheid van deze beeldbemonstering (spatiele discretisatie) wordt bepaald door de resolutie van de CCD sensor en de optiek (lenzen etc.) van de scanner.

In een aantal situaties kan het nodig zijn dat de informatie van het ingescande origineel met een andere informatiedichtheid te verwerken. Een voorbeeld hiervan is het uitvergroten van originelen of het converteren van de resolutie van de CCD sensor naar de resolutie van een printer in een digitale copier. Deze processen hebben de verzamelnaam 'resolutie conversie'. Over het algemeen gebruikt men voor dit doel verschillende soorten algorithmen die de digitaal opgeslagen beeldinformatie bewerken. Resolutie conversie kan in principe ook gedeeltelijk plaatsvinden voordat de beeldinformatie digitaal wordt opgeslagen.

In dit geval moeten de puls-amplitude gemoduleerde uitgangssignalen geconverteerd worden (interpoleren) in een 'glad' (tijds-)continu signaal dat de oorspronkelijke beeldinformatie benadert. Zogenaamde 're-sampling' op bemonsterings frequenties anders dan de klokfrequentie van het tijddiscrete CCD signaal, word dan mogelijk. Gebruik makend van deze mogelijkheden kunnen bijvoorbeeld uitvergrotingen van ingescande afbeeldingen gemaakt worden door meer samples van dit 'gladde' CCD signaal te nemen.

Voor het interpoleren van CCD signalen is een analoog laagdoorlaat filter ontworpen. Een belangrijke eigenschap van dit filter is een bijna lineaire fase karakteristiek (binnen een opgegeven bandbreedte). Hierdoor blijft de vorm van spatiele beeldinformatie ( randovergangen ) zoveel mogelijk behouden. Ook heeft het filter een redelijk scherpe 'roll off' in de amplitude karakteristiek. Hierdoor worden frequentie componenten, in het CCD signaal, die boven de (spatiele) Nyquist frequentie liggen, sterk onderdrukt. 'Ringing' effecten ten gevolge van een te steile 'roll off' worden hierbij vermeden. Het filterontwerp is van een eenvoudige ladderstructuur en kan met goedkope componenten opgebouwd worden. Een nadeel is de gedeeltelijke onderdrukking van frequentie componenten vlak onder de Nyquist frequentie. Hierdoor treedt een zeker verlies in scherpte van ingescande originelen op. Naast de voordelen, zoals het mogelijk worden van 're-sampling' in het analoge domein, worden ook hoogfrequente ruiscomponenten in het CCD signaal onderdrukt en hoeven bijvoorbeeld minder hoge eisen aan de bandbreedte van versterkerschakelingen voor de A/D converter gesteld te worden.

"De schrijver / schrijfster werd door Océ-Nederland B.V. in staat gesteld een onderzoek te verrichten, dat mede aan dit rapport ten grondslag ligt.

Océ-Nederland B.V. aanvaardt geen verantwoordelijkheid voor de juistheid van de in dit rapport vermelde gegevens, beschouwingen en conclusies, die geheel voor rekening van de schrijver / schrijfster komen".